



Università degli Studi di Cagliari
Facoltà di Scienze
Corso di Laurea in Matematica



*On theoretical and numerical
properties of solutions to a
Keller-Segel system*

RELATORI[#]

Prof. Giuseppe Viglialoro
Prof. Rafael Rodríguez Galván

STUDENTESSA

Elena Floris

Anno Accademico 2017-2018

[#]Come beneficiaria di una borsa Erasmus (Progetto Erasmus Plus), la studentessa ha sviluppato parte di questa tesi presso la *Universidad de Cádiz* (UCA-Spagna).

Contents

1	Introduction and motivations	1
1.1	Derivation of the Keller-Segel model	3
1.2	Chemotaxis models: overview and known results	5
2	Lower bounds for the blow-up time in a model of chemotaxis: the two- and three-dimensional cases	7
2.1	Lower bounds for the blow-up time in a Keller-Segel model	7
2.1.1	Conservation mass property	8
2.1.2	Blow-up time in \mathbb{R}^3	9
2.1.3	Blow-up time in \mathbb{R}^2	12
2.2	Lower bounds for the blow-up time in a Keller-Segel system with time dependent coefficients	13
3	Numerical resolution method for the Keller–Segel system	19
3.1	Semi-discretization in space	19
3.2	Numerical tests for $n = 2$	20
3.2.1	Tests with time and space dependent coefficients	21
3.2.2	Tests with constant coefficients	26
3.2.3	Test with negative k_1 coefficient	32
4	General conclusions and future works	40
	Bibliography	41
A	Some essential results on theoretical analysis	45
A.1	Overview on the L^p spaces	45
A.1.1	Definition and elementary properties of L^p spaces: main inequalities	45
A.2	Sobolev spaces: definitions and elementary properties of $W^{1,p}(\Omega)$	46
A.2.1	The space $W_0^{1,p}$	47
A.2.2	Some Sobolev type inequalities	47
B	Some essential results on numerical analysis	49
B.1	Numerical methods for parabolic equations	49
B.2	Variational formulation	49
B.3	Finite difference methods for the 1-D heat equation	50
B.3.1	The forward Euler method	50
B.3.2	The backward Euler method	51
B.4	Finite element method: semidiscretization in space	52
B.5	Finite element method: semidiscretization in time	52
C	Numerical algorithm: a specific case	54

CONTENTS

Chapter 1

Introduction and motivations

Chemotaxis (from chemo + taxis) is the movement of an organism in response to a chemical stimulus. Somatic cells, bacteria, and other single-cell or multicellular organisms direct their movements according to certain chemicals in their environment. This is important for bacteria to find food (glucose) by swimming toward the highest concentration of food molecules, or to flee from poisons (phenol). In multicellular organisms, chemotaxis is critical to early development (movement of sperm towards the egg during fertilization) and subsequent phases of development (migration of neurons or lymphocytes) as well as in normal functions and health (migration of leukocytes during injury or infection). In addition, it has been recognized that mechanisms that allow chemotaxis in animals can be subverted during cancer metastasis.

Positive chemotaxis occurs if the movement is toward a higher concentration of the chemical in question; negative chemotaxis if the movement is in the opposite direction. The description of chemotaxis was first given by T. W. Engelmann (1881) and W.F. Pfeffer (1884) in bacteria and H.S. Jennings (1906) in ciliates (see [17]). The significance of chemotaxis in biology and clinical pathology was widely accepted in the 1930s. The most fundamental definitions belonging to the phenomenon were also drafted by this time. The most important aspects in quality control of chemotaxis assays were described by H.Harris in the 1950s (see Figure 1.1).

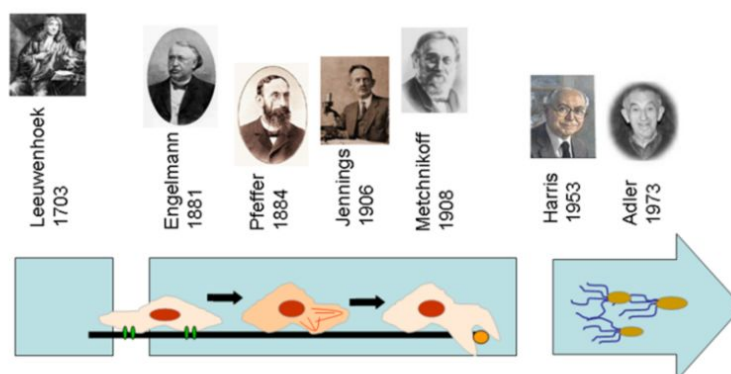


Figure 1.1: Milestones in chemotaxis research.

CHAPTER 1. INTRODUCTION AND MOTIVATIONS

However, to talk about the modern chemotaxis, which started with the revolution of technology, the well-known Keller-Segel model (KS model) should be introduced. Theoretical and mathematical modeling of chemotaxis dates to the works of Patlak in the 1950s and Keller and Segel in the 1970s (see [18]). The general form of the model is given by two coupled PDE's

$$\begin{cases} u_t = \nabla(k_1(u, v)\nabla u - k_2(u, v)u\nabla v) + k_3(u, v), \\ v_t = D_v\Delta v + k_4(u, v) - k_5(u, v)v, \end{cases} \quad (1.1)$$

where $u = u(\mathbf{x}, t)$ and $v = v(\mathbf{x}, t)$ are functions defined in all points \mathbf{x} in the 3D space and instant of time t that denote respectively the cell density and the concentration of the chemical signal, k_1 is the diffusion of the cells, k_2 is the chemotactic sensitivity, k_3 describes the cell growth and death. In signal concentration model, k_4 and k_5 describe the production and degradation of the chemical signal. Note that cell migration is dependent on the gradient of the signal.

The above model has been widely used for chemotaxis for its ability to capture key phenomena and intuitive nature. For example, some bacteria, such as *E. coli*, have several flagella per cell (410 typically). These can rotate in two ways:

- Counter-clockwise rotation aligns the flagella into a single rotating bundle, causing the bacterium to swim in a straight line; and
- Clockwise rotation breaks the flagella bundle apart in such a way each flagellum points in a different direction, causing the bacterium to tumble in place.

The directions of rotation are given for an observer outside the cell looking down the flagella toward the cell (see Figure 1.2).

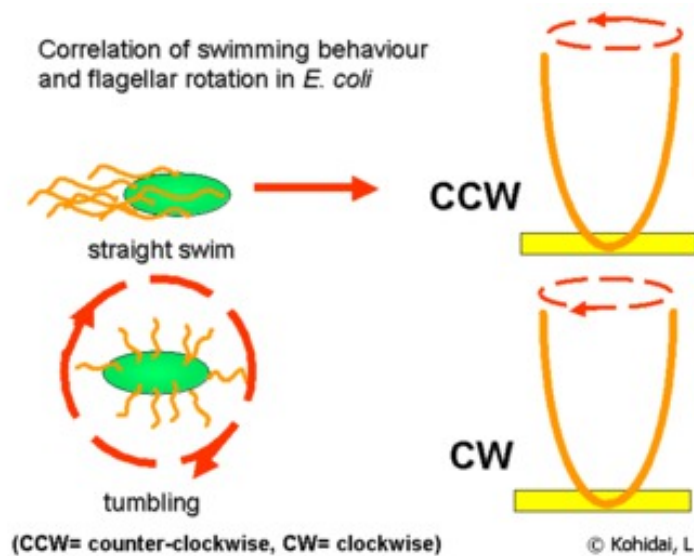


Figure 1.2: Correlation of swimming behaviour and flagellar rotation in *E. coli*

The overall movement of a bacterium is the result of alternating tumble and swim phases. If one watches a bacterium swimming in a uniform environment, its movement will look like a random walk with relatively straight swims interrupted by random tumbles that reorient the bacterium. Bacteria such as *E. coli* are unable to choose the direction in which they swim, and are unable to swim in a straight line for more than a few seconds due to rotational diffusion; in other words, bacteria “forget” the direction in which they are going to. By repeatedly evaluating their course, and adjusting it if they are moving in

CHAPTER 1. INTRODUCTION AND MOTIVATIONS

the wrong direction, bacteria can direct their motion to find favorable locations with high concentrations of attractants (usually food) and avoid repellents (usually poisons).

In the presence of a chemical gradient bacteria will chemotax, or direct their overall motion based on the gradient. If the bacterium senses that it is moving in the correct direction (toward attractant/away from repellent), it will keep swimming in a straight line for a longer time before tumbling; however, if it is moving in the wrong direction, it will tumble sooner and try a new direction at random. In other words, bacteria like *E. coli* use temporal sensing to decide whether their situation is improving or not, and in this way, they find the location with the highest concentration of attractant (usually the source) quite well. Even under very high concentrations, it can still distinguish very small differences in concentration, and fleeing from a repellent works with the same efficiency.

This biased random walk is the result of simply choosing between two methods of random movement; namely tumbling and straight swimming. In fact, chemotactic responses such as forgetting direction and choosing movements resemble the decision-making abilities of higher life-forms with brains that process sensory data.

The helical nature of the individual flagellar filament is critical for this movement to occur, and the protein that makes up the flagellar filament, flagellin, is quite similar among all flagellated bacteria. Vertebrates seem to have taken advantage of this fact by possessing an immune receptor designed to recognize this conserved protein.

As in many instances in biology, there are bacteria that do not follow this rule. Many bacteria, are monoflagellated and have a single flagellum at one pole of the cell. Their method of chemotaxis is different. Others possess a single flagellum that is kept inside the cell wall. These bacteria move by spinning the whole cell, which is shaped like a corkscrew.

The mechanism of chemotaxis that eukaryotic cells employ is quite different from the one which occurs in bacteria; however, sensing of chemical gradients is still a crucial step in the process. Due to their small size, prokaryotes cannot directly detect a concentration gradient. Instead, prokaryotes sense their environments temporally, constantly swimming and redirecting themselves each time they sense a change in the gradient. Eukaryotic cells are much larger than prokaryotes and have receptors embedded uniformly throughout the cell membrane. Eukaryotic chemotaxis involves detecting a concentration gradient spatially by comparing the asymmetric activation of these receptors at the different ends of the cell. Activation of these receptors results in migration towards chemoattractants, or away from chemorepellants.

By utilizing the Keller-Segel model, we can also understand whether chemotaxis may underpin embryonic pattern forming processes (formation of specialized cells, tissues and organs from a single cell, the zygote), such as the formation of the primitive streak, pigmentation patterning in snakes, for example, or zebras. We can also predict the tumor cell-induced angiogenesis, and macrophage invasion into tumor.

1.1 Derivation of the Keller-Segel model

We start deriving the Keller-Segel model from a very basic assumption by letting an arbitrary surface S enclosing a volume V (see [16]), that we denote respectively with $\partial\Omega$ and $\Omega \subset \mathbb{R}^3$. According to the general conservation equation, the rate of change of the amount of material u in Ω equals the rate of flux of u across $\partial\Omega$ out of Ω plus the u created/disappeared in Ω . Thus we have

$$\frac{\partial}{\partial t} \int_{\Omega} u d\mathbf{x} = - \int_{\partial\Omega} \Phi \cdot n ds + \int_{\Omega} f d\mathbf{x},$$

where Φ is the flux of u and f is the source term of u . According to the divergence theorem (see 2.2), the first term on the right results

$$\int_{\partial\Omega} \Phi \cdot n ds = \int_{\Omega} \nabla \cdot \Phi d\mathbf{x},$$

CHAPTER 1. INTRODUCTION AND MOTIVATIONS

and since the function of the cell density u is continuous, and the volume Ω is arbitrary, the integrand must be zero. Thus, the equation can be rewritten as

$$\int_{\Omega} (u_t + \nabla \cdot \Phi - f) d\mathbf{x} = 0,$$

and then simplified the into

$$u_t = -\nabla \cdot \Phi + f. \quad (1.2)$$

This equation holds for a general flux transport Φ whether by diffusion or by some other processes. Since the flux in our chemotaxis model is the contribution of two different terms, which are cell diffusion flux and chemotaxis flux, that is

$$\Phi_{total} = \Phi_{diff} + \Phi_{chemo}.$$

Now, if Fick's law is considered, for the process of cell diffusion flux we write

$$\Phi_{diff} = -D_1 \nabla u,$$

where D_1 is a positive constant, and for the chemotaxis flux,

$$\Phi_{chemo} = \chi u \nabla v,$$

where χ is chemotactic coefficient.

Now, plugging the Φ_{total} into equation (1.2) and repeating the same process above, for the chemical attractant, yields

$$u_t = D_1 \Delta u - \nabla \cdot \chi u(u, v) \nabla v + f(u, v) \quad \text{in } \Omega \times (0, \infty), \quad (1.3)$$

$$v_t = D_2 \Delta v + g(u, v) - h(u, v) \quad \text{in } \Omega \times (0, \infty). \quad (1.4)$$

Moreover, we will fix zero flux boundary conditions(isolated domain), i.e.,

$$\frac{\partial u}{\partial n} = \frac{\partial v}{\partial n} = 0, \quad (1.5)$$

in $\Omega \times (0, \infty)$, where $\frac{\partial}{\partial n}$ stands for the normal derivative on $\partial\Omega$, non negative functions u and v , i.e.

$$u(\mathbf{x}, 0) = u_0(\mathbf{x}) \geq 0, \quad v(\mathbf{x}, 0) = v_0(\mathbf{x}) \geq 0. \quad (1.6)$$

The mentioned Keller-Segel model is still too complicated to solve and to simulate the cell behavior. We need to simplify our model and we come up with a minimal model(see [21]); necessary assumptions are:

- Individual cells undergo a combination of random motion and chemotaxis towards chemical attractant.
- Cell neither die nor divide.
- The attractant is produced at constant rate.
- The degradation rate attractant is linearly dependent on its concentration.
- The attractant diffuses passively over the field.

Using these assumptions, the cell proliferation/death term $f(u, v)$ of equation (1.3) is now zero, the term $g(u, v)$ in the equation (1.4) is now only a function of u ($g(u)$), and the term $h(u, v)$ in the equation (1.4) is now only a function of v that regulates the degradation rate of chemical attractant. Taking D_1 , D_2 , and χ also be positive constant, that represent respectively, the diffusion coefficient of cell, the diffusion coefficient of chemical attractant and the chemotactic sensitivity, the parabolic quasi-linear equation can be noted as:

$$\begin{cases} u_t = D_1 \Delta u - \chi \nabla \cdot (u \nabla v), \\ v_t = D_2 \Delta v + g(u) - h(v), \end{cases} \quad (1.7)$$

with the same conditions (1.5) and (1.6).

1.2 Chemotaxis models: overview and known results

Systems of interacting agents are largely distributed in the physical and biological sciences, from predator-prey models, to taxis-driven pattern formation and front propagation in mathematical biology. The seminal papers by Keller and Segel ([21] and [22]), describe the bacterial chemotaxis, phenomenon in which certain individual cells $u = u(\mathbf{x}, t)$ direct their motion towards a chemical signal $v = v(\mathbf{x}, t)$. A quite general mathematical formulation of these models involves two coupled partial differential equations of the form

$$\begin{cases} u_t = \nabla \cdot (A(u, v)\nabla u - B(u, v)\nabla v) + C(u, v) & \text{in } \Omega \times (0, \infty), \\ \tau v_t = \Delta v + E(u, v) & \text{in } \Omega \times (0, \infty), \\ \frac{\partial u}{\partial \nu} = \frac{\partial v}{\partial \nu} = 0 & \text{in } \partial\Omega \times (0, \infty), \\ u(\mathbf{x}, 0) = u_0(\mathbf{x}) \geq 0 \text{ and } v(\mathbf{x}, 0) = v_0(\mathbf{x}) \geq 0 & \mathbf{x} \in \Omega, \end{cases} \quad (1.8)$$

where $\Omega \subset \mathbb{R}^n$, with $n \geq 1$, is a bounded domain with smooth boundary, $\tau \in \{0, 1\}$ and A, B, C and E are functions of their arguments which depending on the problem are required to satisfy suitable regularity assumptions. Additionally, $u_0(\mathbf{x})$ and $v_0(\mathbf{x})$ are the initial cell and chemical distributions, and $\frac{\partial}{\partial \nu}$ is the outward normal derivative on $\partial\Omega$; in particular, the zero-flux boundary conditions on both u and v indicate that no interaction with the exterior part of the domain is permitted.

For $\tau = 1$, $A(u, v) \equiv 1$, $B(u, v) = \chi u$, with $\chi > 0$, $C(u, v) \equiv 0$, two pioneer cases of the previous system, widely investigated in the last decades, correspond to the choices $E(u, v) = -uv$ and $E(u, v) = -v + u$. While for positive chemical and cell distributions, the negative term $-uv$ in the second equation of (1.8) suggests that the signal is progressively consumed by the same cells, conversely the expression $-v + u$ manifests how an increase of the cells favors a production of the signal. For this latter case a very comprehensive and extensive theory on existence and properties of global, uniformly bounded or blow-up solutions (those that become unbounded in finite or infinite time), especially in terms of the size of the initial data u_0 and v_0 , is available; for a complete picture, we suggest the introduction of [19] for the parabolic-parabolic case (i.e., $\tau = 1$), [32] and [20] for parabolic-elliptic case (i.e., $\tau = 0$) and in addition the survey by [16, Hillen and Painter] where, inter alia, reviews of various models about Keller-Segel-type systems are discussed.

A part from the size of the initial data, the existence of both bounded or unbounded solutions to chemotaxis-systems like (1.8) is an issue also tied to the presence of the source term $C(u, v)$ and/or the mutual interplay between the diffusion $A(u, v)$ and the chemotactic sensitivity $B(u, v)$, also in terms of the space dimension: let us briefly give some information in this regard. First we wish to cite recent contributions (as before all focusing on the linear diffusion case $A(u, v) \equiv 1$, and $B(u, v) = \chi u$) dealing with existence, blow-up and properties of solutions to the fully parabolic version of (1.8) when perturbed by some *logistic-type* effects as $C(u, v) \simeq ku - \mu u^\delta$, for $k \in \mathbb{R}$, $\mu > 0$ and $\delta > 1$: [44], [46],[23], [47] and references therein. Secondly, as far as the relation between $A(u, v)$ and $B(u, v)$ is concerned, the problem with $A(u, v) = (u + 1)^{m-1}$ and $B(u, v) = u(u + 1)^{\alpha-1}$, for some $\alpha, m \in \mathbb{R}$, $C(u, v) \equiv 0$ and $E(u, v) = -v + u$, has been studied in [11], [12] and [43], where it is essentially established that the relation $\alpha < m + \frac{2}{n} - 1$ is a necessary and sufficient condition to ensure global existence and boundedness of solutions even emanating from large initial data. Let us note that the relation mentioned above somehow establishes that the destabilizing effect of the chemo-sensitivity $B(u, v)$ is weaker than that from the diffusion $A(u, v)$, which conversely tends to provide equilibrium to the model.

In this paper $C(u, v)$ will be assumed to be zero, whilst we will dedicate to continuous models comprising specific expressions for the diffusion and the chemotactic sensitivity and that idealize more natural situations than those with $A(u, v) = 1$ and $B(u, v) = \chi u$ (essentially corresponding to the few realistic diffusion with infinite speed of propagation). To be precise, and with the aim of presenting and motivating our investigation, by means of asymptotic methods and the underlying description at the scale of cells at the microscopic level (see [4] and [6]), the cell-cell interaction may even lead to formulations for $A(u, v)$ and $B(u, v)$ capable of modelling the effect that small changes in a stimulus modify the response of a biological agent more heavily at a low signal level than the same changes would in the presence of

CHAPTER 1. INTRODUCTION AND MOTIVATIONS

high signal concentration. In this direction, the signal-dependent sensitivity prototype

$$B(u, v) = \frac{\chi_0}{v}u, \quad v > 0, \quad \text{with some } \chi_0 > 0,$$

which covers the interest of our research, has a particular importance and is employed in the so-called Weber-Fechner law. This law expresses the relation between the actual change in the stimulus and the perceived change, and we suggest [41, 40] for deeper insights and details.

As to previous achievements regarding system (1.8) with singular chemo-sensitivity, results on global existence for initial-boundary value problems with widely arbitrary initial data have been derived in the one-dimensional setting for $A(u, v)$ positive constant and $B(u, v) = \frac{\chi u}{v}$, $\chi > 0$, $C(u, v) \equiv 0$, $\tau = 1$ and $E(u, v) = -uv$ (see [42]). Moreover, with the same choices for $\tau, C(u, v)$ and $E(u, v)$, in [26] and [24], with respectively $A(u, v) \geq \delta u^{m-1}$, $\delta > 0$, and $B(u, v) = \frac{u}{v}$, and $A(u, v) \equiv 1$ and $B(u, v) \simeq \frac{\lambda u(u+1)^{\alpha-1}}{v}$, $\lambda > 0$, for proper values of m and α also in terms of the dimension n , analysis concerning with global classical solutions have been developed as well.

Further, a well established mathematical analysis of this elliptic case of (1.8)

$$\begin{cases} u_t = \Delta u - \nabla \cdot (u\chi(v)\nabla v) & \text{in } \Omega \times (0, \infty), \\ 0 = \Delta v - v + u & \text{in } \Omega \times (0, \infty), \\ \frac{\partial u}{\partial \nu} = \frac{\partial v}{\partial \nu} = 0 & \text{in } \partial\Omega \times (0, \infty), \\ u(\mathbf{x}, 0) = u_0(\mathbf{x}) \geq 0 & \mathbf{x} \in \Omega, \end{cases} \quad (1.9)$$

is available in the literature:

- for $\chi(v) = \frac{\chi_0}{v}$, global existence of weak solutions under the assumption $0 < \chi_0 < \frac{n}{2}$ is proved in [7, Biler];
- for $\chi(v) = \frac{\chi_0}{v}$, uniform boundedness and blow-up of *radial* solutions are positive addressed in [33, Nagai and Senba]; more exactly, solutions are global and remain bounded when either $n \geq 3$ and $0 < \chi_0 < \frac{n}{n-2}$ or $n = 2$ and $\chi_0 > 0$ is arbitrary, whilst for $n \geq 3$, $0 < \chi_0 < \frac{n}{n-2}$ and $\int_{\Omega} u_0 |\mathbf{x}|$ is sufficiently small, the solution blows-up in finite time;
- for $0 < \chi(v) \leq \frac{\chi_0}{v^k}$, with $k \geq 1$ and $v > 0$, global existence and uniform boundedness of classical *nonradial* solutions are discussed in [15, Fujie et al.], where it is shown that the system possesses a unique global classical solution that is uniformly bounded if $0 < \chi_0 < \frac{2}{n}$ ($k = 1$) and $0 < \chi_0 < \frac{2}{n} \frac{k^k}{(k-1)^{k-1}} \gamma^{k-1}$ ($k > 1$), where $\gamma > 0$ is a constant depending on Ω and u_0 .

Chapter 2

Lower bounds for the blow-up time in a model of chemotaxis: the two- and three-dimensional cases

In this manuscript we are interested in chemotactic collapse, a phenomenon connected to the model (1.7). It is experimentally observed that the bacteria may concentrate in one or more points. On the other hand, as discussed in [9] and [10], the so called isothermal collapse (related to relativistic or ultra-cold gases) represents another possible singular scenario.

From a mathematical point of view, the collapse corresponds to the blow-up of the solution at some finite time t^* . In this sense, the blow-up phenomena of solutions to various problems, particularly for nonlinear parabolic systems, have received considerable attention (see, [36], [27], [28], [30], [31]).

In this chapter we derive a lower bound for the blow-up time for the more general parabolic-parabolic system (1.7) choosing: $D_1 = 1$, $g(u) = k_4u$, $h(v) = k_3v$, $D_2 = k_2$, $\chi = k_1$, where k_i ($i = 1, 2, 3, 4$) are positive constants in the section 2.1 and later, in the section 2.2 we making the latter dependent on the time.

Throughout the paper we will often rely on the well known

Proposizione 2.1 (The Divergence Theorem). *Let Ω be a bounded domain of \mathbb{R}^n , $n \geq 1$, and φ a regular function defined on Ω and \mathbf{h} a regular field on Ω . Then*

$$\int_{\Omega} \mathbf{h} \cdot \nabla \varphi d\mathbf{x} = \int_{\partial\Omega} \mathbf{h} \cdot \varphi n - \int_{\Omega} \varphi \nabla \cdot \mathbf{h}. \quad (2.1)$$

In particular, if $\mathbf{h} \cdot n = 0$ on the boundary, we have

$$\int_{\Omega} \mathbf{h} \cdot \nabla \varphi d\mathbf{x} = - \int_{\Omega} \varphi \nabla \cdot \mathbf{h}. \quad (2.2)$$

Proof. See [34]. □

Additionally other usual concepts often employed in analysis will be as well considered; these concepts are summarized in Appendix §A.

2.1 Lower bounds for the blow-up time in a Keller-Segel model

We focus our attention on lower bounds and blow-up times of unbounded classical solutions of problem (1.7). The form of the system is therefore the following:

$$\begin{cases} u_t = \Delta u - k_1 \nabla \cdot (u \nabla v), \\ v_t = k_2 \Delta v - k_3 v + k_4 u, \end{cases} \quad (2.3)$$

CHAPTER 2. LOWER BOUNDS FOR THE BLOW-UP TIME IN A MODEL OF CHEMOTAXIS:
THE TWO- AND THREE-DIMENSIONAL CASES

in $\Omega \times (0, t^*)$ where t^* is the time of blow-up, Ω is a bounded convex region in either \mathbb{R}^2 or \mathbb{R}^3 with smooth boundary $\partial\Omega$, and $k_i (i = 1, 2, 3, 4)$ are positive constants. Associated with the boundary conditions

$$\frac{\partial u}{\partial n} = \frac{\partial v}{\partial n} = 0, \quad (2.4)$$

in $\Omega \times (0, t^*)$, where $\frac{\partial}{\partial n}$ stands for the normal derivative on $\partial\Omega$. In addition, the non negative functions u and v satisfy the initial conditions

$$u(\mathbf{x}, 0) = u_0(\mathbf{x}) \geq 0, \quad v(\mathbf{x}, 0) = v_0(\mathbf{x}) \geq 0. \quad (2.5)$$

Here u is a continuous function and v is a C^2 function in Ω with v satisfying appropriate compatibility on $\partial\Omega$.

2.1.1 Conservation mass property

A consequence easily derivable from the equations of (2.3) is the so called *conservation mass property* for the u -component. This issue is both mathematically and biologically important, so that we prove it in this

Proposizione 2.2. *Let (u, v) a classical solution to (2.3)-(2.5). Then the u -component satisfies*

$$\int_{\Omega} u(\mathbf{x}, t) d\mathbf{x} = \int_{\Omega} u_0(\mathbf{x}) d\mathbf{x} =: m \quad \forall t > 0. \quad (2.6)$$

As the v -component, we have

$$\int_{\Omega} v(\mathbf{x}, t) d\mathbf{x} \leq L := \max \left\{ \int_{\Omega} v_0(\mathbf{x}), \frac{k_4 m}{k_3} \right\} \quad \forall t > 0. \quad (2.7)$$

Proof. By integrating over Ω the first equation of (2.3) we have

$$\int_{\Omega} u_t d\mathbf{x} = \int_{\Omega} \nabla \cdot \nabla u d\mathbf{x} - k_1 \int_{\Omega} \nabla \cdot (u \nabla v) d\mathbf{x}.$$

Using the Divergence Theorem (see formula (2.2)) and the zero-flux boundary conditions, we have that

$$\int_{\Omega} \nabla \cdot \nabla u d\mathbf{x} = 0 \quad \int_{\Omega} \nabla \cdot (u \nabla v) d\mathbf{x},$$

so that

$$\frac{d}{dt} \int_{\Omega} u d\mathbf{x} = \int_{\Omega} u_t d\mathbf{x} = 0,$$

and hence by virtue of the initial condition $\int_{\Omega} u_0 d\mathbf{x} = m$, we conclude.

On the other hand, since similar arguments applied to v give

$$\frac{d}{dt} \int_{\Omega} v d\mathbf{x} = -k_3 \int_{\Omega} v d\mathbf{x} + k_4 m,$$

we can explicitly solve this linear ordinary differential equation and achieve the second claim. \square

Remark 1. We observe that Proposition 2.2 implies that the quantity $\int_{\Omega} u d\mathbf{x}$ is conserved throughout the time and that $\int_{\Omega} u d\mathbf{x}$ is bounded; in other words both $\|u\|_{L^1(\Omega)}$ and $\|v\|_{L^1(\Omega)}$ are finite; nevertheless, from this interesting property nothing can be deduced on the boundedness of both u and v .

2.1.2 Blow-up time in \mathbb{R}^3

With the aim of proving our main results dealing with estimates of the blow-up time t^* of unbounded classical solutions to (2.3), we have to establish some necessary facts.

We define this auxiliary function to any solution (u, v) as follows:

$$\phi(t) = \alpha \int_{\Omega} u^2 d\mathbf{x} + \int_{\Omega} (\Delta v)^2 d\mathbf{x}, \quad (2.8)$$

whose value at $t = 0$ is

$$\phi(0) = \alpha \int_{\Omega} u_0^2 d\mathbf{x} + \int_{\Omega} (\Delta v_0)^2 d\mathbf{x},$$

where $\alpha > 0$ is a positive constant to be determined.

We also need this

Definition 2.1. *The solution (u, v) to system (2.3) blows-up in ϕ -measure at time t^* if*

$$\lim_{t \rightarrow t^*} \phi(t) = \infty. \quad (2.9)$$

Now we can claim this

Theorem 2.3. *Let (u, v) be the classical solution of (2.3)-(2.5) in a convex region Ω of \mathbb{R}^3 with smooth boundary and compatible data, and suppose the solution blows up in ϕ measure at time t^* . Then t^* satisfies*

$$t^* \geq \int_{\phi(0)}^{\infty} \frac{d\eta}{A\eta^{\frac{3}{2}} + B\eta^3}, \quad (2.10)$$

where A and B are appropriate positive constants.

Proof. To derive a lower bound for t^* , let us differentiate with respect to the time t the auxiliary function given in Definition 2.8: we have

$$\frac{d\phi}{dt} = 2\alpha \int_{\Omega} uu_t d\mathbf{x} + 2 \int_{\Omega} \Delta v \Delta v_t d\mathbf{x}, \quad (2.11)$$

so that replacing u_t with its expression, we achieve

$$= 2\alpha \int_{\Omega} u[\Delta u - k_1 \nabla \cdot (u \nabla v)] d\mathbf{x} + 2 \int_{\Omega} \Delta v \Delta v_t d\mathbf{x}. \quad (2.12)$$

Applying the divergence theorem (see (2.2)) and taking into account the boundary conditions of Neumann we have

$$= -2\alpha \int_{\Omega} |\nabla u|^2 d\mathbf{x} - \alpha k_1 \int_{\Omega} u^2 \Delta v d\mathbf{x} - 2 \int_{\Omega} \nabla(\Delta v) \cdot \nabla v_t d\mathbf{x},$$

and, as before, replacing v_t we have

$$\begin{aligned} &= -2\alpha \int_{\Omega} |\nabla u|^2 d\mathbf{x} - \alpha k_1 \int_{\Omega} u^2 \Delta v d\mathbf{x} - 2 \int_{\Omega} \nabla(\Delta v) \cdot \nabla(k_2 \Delta v - k_3 v + k_4 u) d\mathbf{x} \\ &= -2\alpha \int_{\Omega} |\nabla u|^2 d\mathbf{x} - \alpha k_1 \int_{\Omega} u^2 \Delta v d\mathbf{x} - 2k_2 \int_{\Omega} |\nabla(\Delta v)|^2 d\mathbf{x} - 2k_3 \int_{\Omega} (\Delta v)^2 d\mathbf{x} \\ &\quad - 2k_4 \int_{\Omega} \nabla(\Delta v) \cdot (\nabla u) d\mathbf{x} \\ &\leq -2\alpha \int_{\Omega} |\nabla u|^2 d\mathbf{x} - \alpha k_1 \int_{\Omega} u^2 \Delta v d\mathbf{x} - 2k_2 \int_{\Omega} |\nabla(\Delta v)|^2 d\mathbf{x} - 2k_3 \int_{\Omega} (\Delta v)^2 d\mathbf{x} \end{aligned}$$

CHAPTER 2. LOWER BOUNDS FOR THE BLOW-UP TIME IN A MODEL OF CHEMOTAXIS:
THE TWO- AND THREE-DIMENSIONAL CASES

$$+k_4\varepsilon_1 \int_{\Omega} |\nabla(\Delta v)|^2 d\mathbf{x} + \frac{k_4}{\varepsilon_1} \int_{\Omega} (\nabla u)^2 d\mathbf{x}. \quad (2.13)$$

In the last step, we used Hölder's inequality (see A.1), the inequality

$$a^p b^{1-p} \leq pa + (1-p)b, \quad (2.14)$$

with an undetermined positive weight factor ε_1 .

We now focus our attention on the second term on the right in (2.13) and with the same procedure and an undetermined positive weight factor ε_1 we have

$$\left[\varepsilon_2 \int_{\Omega} u^3 d\mathbf{x} \right]^{\frac{2}{3}} \left[\frac{1}{\varepsilon_2} \int_{\Omega} |\Delta v|^3 d\mathbf{x} \right]^{\frac{1}{3}} \leq \frac{2\varepsilon_2}{3} \int_{\Omega} u^3 d\mathbf{x} + \frac{1}{3\varepsilon_2^2} \int_{\Omega} |\Delta v|^3 d\mathbf{x} \quad (2.15)$$

Substituting (2.15) in (2.13), we have

$$\begin{aligned} \frac{d\phi}{dt} \leq & -2\alpha \int_{\Omega} |\nabla u|^2 d\mathbf{x} - \alpha k_1 \left\{ \frac{2\varepsilon_2}{3} \int_{\Omega} u^3 d\mathbf{x} + \frac{1}{3\varepsilon_2^2} \int_{\Omega} |\Delta v|^3 d\mathbf{x} \right\} - 2k_2 \int_{\Omega} |\nabla(\Delta v)|^2 d\mathbf{x} \\ & - 2k_3 \int_{\Omega} (\Delta v)^2 d\mathbf{x} + k_4\varepsilon_1 \int_{\Omega} |\nabla(\Delta v)|^2 d\mathbf{x} + \frac{k_4}{\varepsilon_1} \int_{\Omega} (\nabla u)^2 d\mathbf{x}, \end{aligned}$$

adding up the terms we have

$$\begin{aligned} \frac{d\phi}{dt} \leq & -2\alpha \int_{\Omega} |\nabla u|^2 d\mathbf{x} - \alpha k_1 \left\{ \frac{2\varepsilon_2}{3} \int_{\Omega} u^3 d\mathbf{x} + \frac{1}{3\varepsilon_2^2} \int_{\Omega} |\Delta v|^3 d\mathbf{x} \right\} \\ & - (2k_2 - k_4\varepsilon_1) \int_{\Omega} |\nabla(\Delta v)|^2 d\mathbf{x} - 2k_3 \int_{\Omega} (\Delta v)^2 d\mathbf{x} + \frac{k_4}{\varepsilon_1} \int_{\Omega} (\nabla u)^2 d\mathbf{x}. \end{aligned} \quad (2.16)$$

To bound the second term on the right in (2.16) in terms of ϕ , $\int_{\Omega} |\nabla u|^2 d\mathbf{x}$ and $\int_{\Omega} \nabla(\Delta v)\nabla(\Delta v) d\mathbf{x}$, we make use of an inequality (2.16) in reference [38], i.e.

$$\int_{\Omega} u^3 d\mathbf{x} \leq \left[m_1 \int_{\Omega} u^2 d\mathbf{x} + m_2 \left(\int_{\Omega} u^2 d\mathbf{x} \right)^{\frac{1}{2}} \left(\int_{\Omega} |\nabla u|^2 d\mathbf{x} \right)^{\frac{1}{2}} \right]^{\frac{3}{2}}. \quad (2.17)$$

Using the fact that for positive a and b we have

$$(a+b)^{\frac{3}{2}} \leq 2^{\frac{1}{2}}(a^{\frac{3}{2}} + b^{\frac{3}{2}}), \quad (2.18)$$

the (2.17) becomes

$$\leq 2^{\frac{1}{2}} \left[m_1^{\frac{3}{2}} \left(\int_{\Omega} u^2 d\mathbf{x} \right)^{\frac{3}{2}} + m_2^{\frac{3}{2}} \left(\int_{\Omega} u^2 d\mathbf{x} \right)^{\frac{3}{4}} \left(\int_{\Omega} |\nabla u|^2 d\mathbf{x} \right)^{\frac{3}{4}} \right],$$

so that using Hölder's inequality and (2.14), with a positive and unspecified weight ε_3 , we obtain that

$$\leq 2^{\frac{1}{2}} \left\{ m_1^{\frac{3}{2}} \left(\int_{\Omega} u^2 d\mathbf{x} \right)^{\frac{3}{2}} + m_2^{\frac{3}{2}} \left[\frac{1}{4\varepsilon_3^3} \left(\int_{\Omega} u^2 d\mathbf{x} \right)^3 + \frac{3\varepsilon_3}{4} \int_{\Omega} |\nabla u|^2 d\mathbf{x} \right] \right\}, \quad (2.19)$$

where we have used (2.14) and

$$m_1 = \frac{1}{2 \cdot 3^{\frac{1}{8}} p_0}, \quad m_2 = \frac{1}{3^{\frac{9}{8}} p_0} \left(\frac{d}{p_0} + 1 \right),$$

CHAPTER 2. LOWER BOUNDS FOR THE BLOW-UP TIME IN A MODEL OF CHEMOTAXIS:
THE TWO- AND THREE-DIMENSIONAL CASES

and for some origin inside Ω

$$p_0 = \max_{\partial\Omega} \mathbf{x}_i n_i > 0, \quad d^2 = \max_{\Omega} \mathbf{x}_i \mathbf{x}_i,$$

n_i being the i -th component of the unit normal vector directed outward on $\partial\Omega$.

Similarly, using the reference [38]

$$\int_{\Omega} |\Delta v|^3 \leq 2^{\frac{1}{2}} \left\{ m_1^{\frac{3}{2}} \left(\int_{\Omega} \Delta v^2 d\mathbf{x} \right)^{\frac{3}{2}} + m_2^{\frac{3}{2}} \left[\frac{1}{4\varepsilon_3^4} \left(\int_{\Omega} (\Delta v)^2 d\mathbf{x} \right)^3 + \frac{3\varepsilon_4}{4} \int_{\Omega} |\nabla(\Delta v)|^2 d\mathbf{x} \right] \right\}. \quad (2.20)$$

Substituting (2.19) and (2.20) into (2.16), we obtain the differential inequality

$$\begin{aligned} \frac{d\phi}{dt} \leq & \left[-2\alpha + \frac{1}{\sqrt{2}} m_2^{\frac{3}{2}} k_1 \alpha \varepsilon_2 \varepsilon_3 + \frac{k_4}{\varepsilon_1} \right] \int_{\Omega} |\nabla u|^2 d\mathbf{x} + \left[-2k_2 + k_4 \varepsilon_1 + \sqrt{2} k_1 \alpha m_2^{\frac{3}{2}} \frac{\varepsilon_4}{4\varepsilon_2^2} \right] \int_{\Omega} |\nabla(\Delta v)|^2 d\mathbf{x} \\ & + \frac{2}{3} k_1 \alpha \varepsilon_2 \left[\sqrt{2} m_1^{\frac{3}{2}} \left(\int_{\Omega} u^2 d\mathbf{x} \right)^{\frac{3}{2}} + \frac{\sqrt{2} m_2^{\frac{3}{2}}}{4\varepsilon_3^3} \left(\int_{\Omega} u^2 d\mathbf{x} \right)^3 \right] + \frac{\sqrt{2} k_1 \alpha m_1^{\frac{3}{2}}}{3\varepsilon_2^2} \left[\int_{\Omega} (\Delta v)^2 d\mathbf{x} \right]^{\frac{3}{2}} \\ & + \frac{\sqrt{2} k_1 \alpha m_2^{\frac{3}{2}}}{12\varepsilon_2^2 \varepsilon_4^3} \left[\int_{\Omega} (\Delta v)^2 d\mathbf{x} \right]^3 - 2k_3 \int_{\Omega} (\Delta v)^2 d\mathbf{x}. \end{aligned} \quad (2.21)$$

We drop the last term on the right side and choose α and the ε_i ($i = 1, 2, 3, 4$) such that

$$\begin{aligned} -2\alpha + \frac{1}{\sqrt{2}} m_2^{\frac{3}{2}} k_1 \alpha \varepsilon_2 \varepsilon_3 + \frac{k_4}{\varepsilon_1} &\leq 0, \\ -2k_2 + k_4 \varepsilon_1 + \sqrt{2} k_1 \alpha m_2^{\frac{3}{2}} \frac{\varepsilon_4}{4\varepsilon_2^2} &\leq 0, \end{aligned}$$

and arrive at

$$\frac{d\phi}{dt} \leq A\phi^{\frac{3}{2}} + B\phi^3, \quad (2.22)$$

where A and B are computable constants depending on the choices made for α and the ε_i . A possible choice for α and the ε_i is

$$\begin{aligned} \varepsilon_1 &= \frac{k_2}{k_4}, \varepsilon_2 = 1, \\ \varepsilon_3 &= \frac{\sqrt{2}}{k_1 m_2^{\frac{3}{2}}}, \varepsilon_4 = \frac{2\sqrt{2} k_2^2}{k_1 k_4^2 m_2^{\frac{3}{2}}}, \alpha = \frac{k_4^2}{k_2}. \end{aligned}$$

An integration of (2.22) leads to

$$t \geq \int_{\phi(0)}^{\phi(t)} \frac{d\eta}{A\eta^{\frac{3}{2}} + B\eta^3},$$

and if $\phi(t)$ blow-up at time t^* then

$$t^* \geq \int_{\phi(0)}^{\infty} \frac{d\eta}{A\eta^{\frac{3}{2}} + B\eta^3}, \quad (2.23)$$

where

$$\phi(0) = \alpha \int_{\Omega} u_0^2 d\mathbf{x} + \int_{\Omega} (\Delta v_0)^2 d\mathbf{x}.$$

□

CHAPTER 2. LOWER BOUNDS FOR THE BLOW-UP TIME IN A MODEL OF CHEMOTAXIS:
THE TWO- AND THREE-DIMENSIONAL CASES

Remark 2. Let us underline these details:

- The convexity in \mathbb{R}^3 was used in the derivation of (2.19). However, the derivation of the theorem requires only that Ω be star shaped and convex separately in two orthogonal directions, so our result holds for these more general regions.
- The integral (2.23) can either be evaluated or easily bounded from below. It is also useful to notice that if it is not known whether the solution blows up or not, our bound will assure us of a safe time period in which blow-up cannot occur.

2.1.3 Blow-up time in \mathbb{R}^2

In a similar way we establish this

Theorem 2.4. *Let (u, v) be the solution of (2.3)-(2.5) in a convex region D in \mathbb{R}^2 with smooth boundary and compatible data, and suppose that solution blows up in ϕ -measure (2.8) at time t^* . Then for some positive and computable constants A_1 and B_1 , t^* satisfies*

$$t^* \geq \int_{\phi(0)}^{\infty} \frac{d\eta}{A_1 \eta^{\frac{3}{2}} + B_1 \eta^2}.$$

Proof. The arguments through (2.13) apply as before. However, (2.14) and (2.20) will be changed. In the derivation of (2.16) in [38], the authors make use of an inequality, which in our notation is

$$\left(\int_D u^4 dA \right)^{\frac{1}{2}} \leq \left(\frac{1}{2} \oint_{\partial D} u^2 |n_x| ds + \int_D u |u_{,x}| dA \right)^{\frac{1}{2}} \times \left(\frac{1}{2} \oint_{\partial D} u^2 |n_y| ds + \int_D u |u_{,y}| dA \right)^{\frac{1}{2}}, \quad (2.24)$$

using (2.14) we have:

$$\left(\int_D u^4 dA \right)^{\frac{1}{2}} \leq \frac{1}{4} \left(\oint_{\partial D} u^2 |n_x| ds + \oint_{\partial D} u^2 |n_y| ds \right) + \frac{1}{2} \left(\int_D u |u_{,x}| dA + \int_D u |u_{,y}| dA \right),$$

and using the Cauchy-Schwartz inequality (see (A.1)) we have:

$$\begin{aligned} &\leq \frac{1}{4} \left[\left(\oint_{\partial D} u^2 ds \oint_{\partial D} u^2 |n_x|^2 ds \right)^{\frac{1}{2}} + \left(\oint_{\partial D} u^2 ds \oint_{\partial D} u^2 |n_y|^2 ds \right)^{\frac{1}{2}} \right] \\ &\quad + \frac{1}{2} \left[\left(\int_D u^2 dA \int_D u_x^2 dA \right)^{\frac{1}{2}} + \left(\int_D u^2 dA \int_D u_y^2 dA \right)^{\frac{1}{2}} \right] \\ &\leq \frac{\sqrt{2}}{4} \oint_{\partial D} u^2 ds + \frac{\sqrt{2}}{2} \left(\int_D u^2 dA \right)^{\frac{1}{2}} \left(\int_D |\nabla u|^2 dA \right)^{\frac{1}{2}}, \end{aligned} \quad (2.25)$$

where in the last step we used (2.18).

Again, since D is assumed to be convex, it follows that

$$\oint_{\partial D} u^2 ds \leq \frac{2}{p_0} \int_D u^2 dA + \frac{2d}{p_0} \left(\int_D u^2 dA \int_D |\nabla u|^2 dA \right)^{\frac{1}{2}}, \quad (2.26)$$

where as before

$$p_0 = \min_{\partial \Omega} \mathbf{x}_\beta n_\beta > 0, \quad d^2 = \max_{\Omega} \mathbf{x}_\beta \mathbf{x}_\beta, \quad \beta = 1, 2. \quad (2.27)$$

CHAPTER 2. LOWER BOUNDS FOR THE BLOW-UP TIME IN A MODEL OF CHEMOTAXIS:
THE TWO- AND THREE-DIMENSIONAL CASES

Inserting (2.25) back into (2.26) and making use of the inequality:

$$\int_D u^3 dA \leq \left(\int_D u^2 dA \int_D u^4 dA \right)^{\frac{1}{2}}, \quad (2.28)$$

leads to the bounds

$$\int_D u^3 dA \leq \frac{\sqrt{2}}{2p_0} \left(\int_D u^2 dA \right)^{\frac{3}{2}} + \frac{\sqrt{2}}{2} \left(1 + \frac{d}{p_0} \right) \int_D u^2 dA \left(\int_D |\nabla u|^2 dA \right)^{\frac{3}{2}}, \quad (2.29)$$

and

$$\int_D |\Delta v|^3 dA \leq \frac{\sqrt{2}}{2p_0} \left(\int_D |\Delta v|^2 dA \right)^{\frac{3}{2}} + \frac{\sqrt{2}}{2} \left(1 + \frac{d}{p_0} \right) \int_D |\Delta v|^2 dA \left(\int_D \Delta v \Delta v dA \right)^{\frac{1}{2}}. \quad (2.30)$$

Following the arguments used for \mathbb{R}^3 we arrive at

$$t^* \geq \int_{\phi(0)}^{\infty} \frac{d\eta}{A_1 \eta^{\frac{3}{2}} + B_1 \eta^2}, \quad (2.31)$$

where again the values of A_1 , B_1 and the integral are easily obtainable. \square

2.2 Lower bounds for the blow-up time in a Keller-Segel system with time dependent coefficients

In the previous section we have analyzed a lower bound for the blow-up time of solutions to system (2.3) when Ω is a bounded domain in \mathbb{R}^2 or \mathbb{R}^3 . On the other and, natural observations and practical experiences show how in specific circumstances the parameters modeling the chemotaxis phenomena can also change in time. As a consequence, we are interested in studying a different model, where the positive coefficients in (2.3) are herein replaced by positive time dependent coefficients. Therefore we express the system in the following way

$$\begin{cases} u_t = \Delta u - k_1(t) \nabla \cdot (u \nabla v), & (x, t) \in \Omega \times (0, t^*), \\ v_t = k_2(t) \Delta v - k_3(t) v + k_4(t) u & (x, t) \in \Omega \times (0, t^*), \\ u_n = v_n = 0 & (x, t) \in \partial\Omega \times (0, t^*), \\ u(\mathbf{x}, 0) = u_0(\mathbf{x}) \geq 0, v(\mathbf{x}, 0) = v_0(\mathbf{x}) \geq 0 & x \in \Omega, \end{cases} \quad (2.32)$$

where t^* is the blow-up time ($0 < t^* < \infty$), Ω is the bounded domain in \mathbb{R}^3 with smooth boundary $\partial\Omega$, u_n and v_n are the normal derivative on $\partial\Omega$. , $u_0(\mathbf{x})$ and $v_0(\mathbf{x})$ are assumed non-negative on Ω satisfying the compatibility conditions on $\partial\Omega$.

As mentioned in different places throughout this report, system (2.32) represents the following situation: the chemoattractant spreads diffusively and decays with rate $k_2(t)$ and $k_3(t)$, respectively; it is also produced by the bacteria with rate $k_4(t)$. The bacteria diffuse with mobility 1 and also drift in the direction of the gradient of concentration of the chemoattractant with velocity $k_1(t)|\nabla v|$; k_1 is called chemosensitivity. Moreover, the Neumann boundary conditions mean that no flux with the external boundary is permitted (from now on, we also refer to the so called zero-flux boundary conditions).

We will study solutions of (2.32) which blow-up in finite time t^* . It is well known that when blow-up occurs at t^* , explicit estimates are of a great practical interest, since, mostly, it is not possible an exact computation of t^* . More precisely, we derive sufficient conditions on the data in order to obtain an explicit lower bound for t^* .

Let us present the main result; we first need to introduce the following auxiliary function

$$W(t) = \alpha(t) \int_{\Omega} u^2 d\mathbf{x} + \beta(t) \int_{\Omega} (\Delta v)^2 d\mathbf{x}, \quad (2.33)$$

CHAPTER 2. LOWER BOUNDS FOR THE BLOW-UP TIME IN A MODEL OF CHEMOTAXIS:
THE TWO- AND THREE-DIMENSIONAL CASES

whose value at $t = 0$ is

$$W(0) = \alpha(0) \int_{\Omega} u_0^2 d\mathbf{x} + \beta(0) \int_{\Omega} (\Delta v_0)^2 d\mathbf{x},$$

$\alpha(t)$ and $\beta(t)$ in (2.33) are positive and derivable functions in $[0, t^*)$, to be determined.

Now we give the following definition.

Definition 2.2. *The solution (u, v) to system (2.32) blows-up in W -measure at time t^* if*

$$\lim_{t \rightarrow t^*} W(t) = \infty. \quad (2.34)$$

Now we state our main result, we derive an explicit lower bound for t^* . For brevity we write $k_i := k_i(t)$, $i = 1, 2, 3, 4$.

Theorem 2.5. *Let (u, v) be a classical solution of (2.32). Assume Ω a bounded domain in \mathbb{R}^3 , with the origin inside, star-shaped and convex in two orthogonal directions. Let W defined in (2.33) and (u, v) becomes unbounded at some time t^* in W -measure (2.34). Moreover assume that the coefficients k_i (for $i = 1, 2, 3, 4$) satisfy the following relation*

$$\frac{2k'_4}{k_4} - \frac{k'_2}{k_2} + 2k_3 \leq 0, \quad (2.35)$$

and let be

$$\begin{cases} \beta(t) = \exp^{2K_3(t)}, \text{ with } K_3(t) = \int_0^t k_3(s) d\mathbf{x}, \\ \alpha(t) = \frac{k_4^2}{k_2} \beta \end{cases}$$

Then

$$t^* \geq H^{-1} \left(\frac{1}{2W(0)^2} \right), \quad (2.36)$$

with H^{-1} the inverse function of $H(t) := \int_0^t \omega(\tau)$, $\omega(\tau)$ being a positive function depending only on the data.

Proof. We show that $W(t)$ defined on solution of the system (2.32) satisfies an appropriate differential inequality of the first order. By integrating such inequality we get the lower bound of t^* .

By differentiating $W(t)$ we have

$$W'(t) = \alpha' \int_{\Omega} u^2 d\mathbf{x} + \beta' \int_{\Omega} (\Delta v)^2 d\mathbf{x} + 2\alpha \int_{\Omega} uu_t d\mathbf{x} + 2\beta \int_{\Omega} \Delta v \Delta v_t d\mathbf{x}. \quad (2.37)$$

Now we focus our attention to the last two integrals in (2.37). By using the first equation in (2.32) and the divergence theorem (see 2.2), we can be write

$$\begin{aligned} \int_{\Omega} uu_t d\mathbf{x} &= \int_{\Omega} u [\Delta u - k_1(t) \nabla \cdot (u \nabla v)] d\mathbf{x} \\ &= \int_{\Omega} u \Delta u d\mathbf{x} - k_1(t) \int_{\Omega} u \nabla \cdot (u \nabla v) d\mathbf{x} \\ &= - \int_{\Omega} |\nabla u|^2 d\mathbf{x} - k_1(t) \int_{\Omega} u \nabla \cdot (u \nabla v) d\mathbf{x} \end{aligned}$$

By using

$$\nabla \cdot (u \nabla v) = \nabla u \cdot \nabla v + u \Delta v,$$

and the divergence theorem (see 2.2), we have

$$\int_{\Omega} uu_t d\mathbf{x} = - \int_{\Omega} |\nabla u|^2 d\mathbf{x} + k_1(t) \frac{1}{2} \int_{\Omega} u^2 \Delta v d\mathbf{x}. \quad (2.38)$$

CHAPTER 2. LOWER BOUNDS FOR THE BLOW-UP TIME IN A MODEL OF CHEMOTAXIS:
THE TWO- AND THREE-DIMENSIONAL CASES

Moreover, it can be checked that

$$\int_{\Omega} \Delta v \Delta v_t d\mathbf{x} = \int_{\Omega} \nabla \cdot (\nabla v_t) \Delta v d\mathbf{x} = - \int_{\Omega} \nabla(\Delta v) \cdot \nabla v_t d\mathbf{x},$$

using the second equation in (2.32), we have

$$\begin{aligned} &= - \int_{\Omega} \nabla(\Delta v) \cdot \nabla [k_2(t) \Delta v - k_3(t)v + k_4(t)u] d\mathbf{x} \\ &= -k_2(t) \int_{\Omega} |\nabla(\Delta v)|^2 d\mathbf{x} + k_3(t) \int_{\Omega} \nabla(\Delta v) \cdot \nabla v d\mathbf{x} - k_4(t) \int_{\Omega} \nabla(\Delta v) \cdot \nabla u d\mathbf{x}. \end{aligned} \quad (2.39)$$

We observe that

$$\int_{\Omega} \nabla(\Delta v) \cdot \nabla v d\mathbf{x} = - \int_{\Omega} (\Delta v)^2 d\mathbf{x}. \quad (2.40)$$

Now by using Schwarz's inequality (see (A.1)) and (A.4), we have

$$\begin{aligned} \int_{\Omega} |\nabla(\Delta v)| |\nabla u| d\mathbf{x} &= \left(\epsilon_1 \int_{\Omega} |\nabla(\Delta v)|^2 d\mathbf{x} \right)^{\frac{1}{2}} \left(\frac{1}{\epsilon_1} \int_{\Omega} |\nabla u|^2 d\mathbf{x} \right)^{\frac{1}{2}} \\ &\leq \frac{\epsilon_1}{2} \int_{\Omega} |\nabla(\Delta v)|^2 d\mathbf{x} + \frac{1}{2\epsilon_1} \int_{\Omega} |\nabla u|^2 d\mathbf{x} \end{aligned} \quad (2.41)$$

where ϵ_1 is an arbitrary positive and time depending function to be determined.

We now combine the terms (2.40) and (2.41) in (2.39) and obtain

$$\int_{\Omega} \Delta v \Delta v_t \leq (k_4(t) \frac{\epsilon_1}{2} - k_2(t)) \int_{\Omega} |\nabla(\Delta v)|^2 d\mathbf{x} - k_3(t) \int_{\Omega} (\Delta v)^2 d\mathbf{x} + k_4(t) \frac{1}{2\epsilon_1} \int_{\Omega} |\nabla u|^2 d\mathbf{x}. \quad (2.42)$$

Plugging (2.38) and (2.42) in (2.37) we lead to

$$\begin{aligned} W'(t) &= \alpha' \int_{\Omega} u^2 d\mathbf{x} + \beta' \int_{\Omega} (\Delta v)^2 d\mathbf{x} + \left(-2\alpha + \frac{k_4\beta}{\epsilon_1}\right) \int_{\Omega} |\nabla u|^2 d\mathbf{x} \\ &\quad + \alpha k_1 \int_{\Omega} u^2 \Delta v d\mathbf{x} - 2\beta k_2 \int_{\Omega} |\nabla(\Delta v)|^2 d\mathbf{x} + \epsilon_1 \beta k_4 \int_{\Omega} |\nabla(\Delta v)|^2 d\mathbf{x} - 2k_3\beta \int_{\Omega} (\Delta v)^2 d\mathbf{x} \end{aligned}$$

Regarding term $\int_{\Omega} u^2 \Delta v d\mathbf{x}$, by means of Hölder's inequality and (A.4) we obtain

$$\int_{\Omega} u^2 \Delta v d\mathbf{x} \leq \frac{2\epsilon_2}{3} \int_{\Omega} u^3 d\mathbf{x} + \frac{1}{3\epsilon_2} \int_{\Omega} |\Delta v|^3 d\mathbf{x}, \quad (2.43)$$

with ϵ_2 another positive and time depending function to be chosen.

We observe that we are now under the hypotheses of LemmaA.2, which can be applied to both terms in (2.43). In fact we can write

$$\int_{\Omega} u^3 d\mathbf{x} \leq \sqrt{2} \left[m_1^{\frac{3}{2}} \left(\int_{\Omega} u^2 d\mathbf{x} \right)^{\frac{3}{2}} + m_2^{\frac{3}{2}} \left[\frac{1}{4\epsilon_3^3} \left(\int_{\Omega} u^2 d\mathbf{x} \right)^3 + \frac{3\epsilon_3}{4} \left(\int_{\Omega} |\nabla u|^2 d\mathbf{x} \right) \right] \right], \quad (2.44)$$

and

$$\int_{\Omega} |\Delta v|^3 d\mathbf{x} \leq \sqrt{2} \left[m_1^{\frac{3}{2}} \left(\int_{\Omega} |\Delta v|^2 d\mathbf{x} \right)^{\frac{3}{2}} + m_2^{\frac{3}{2}} \left[\frac{1}{4\epsilon_4^3} \left(\int_{\Omega} |\Delta v|^2 d\mathbf{x} \right)^3 + \frac{3\epsilon_4}{4} \left(\int_{\Omega} |\nabla(\Delta v)|^2 d\mathbf{x} \right) \right] \right], \quad (2.45)$$

CHAPTER 2. LOWER BOUNDS FOR THE BLOW-UP TIME IN A MODEL OF CHEMOTAXIS:
THE TWO- AND THREE-DIMENSIONAL CASES

where ε_3 and ε_4 are any positive and time depending functions to be determined. Hence, by employing (2.45) and (2.44) in (2.43), we have

Then

$$\begin{aligned} \int_{\Omega} u^2 \Delta v dx &\leq \frac{2\varepsilon_2}{3} \sqrt{2} \left[m_1^{\frac{3}{2}} \left(\int_{\Omega} u^2 dx \right)^{\frac{3}{2}} + m_2^{\frac{3}{2}} \left[\frac{1}{4\varepsilon_3^3} \left(\int_{\Omega} u^2 dx \right)^3 + \frac{3\varepsilon_3}{4} \left(\int_{\Omega} |\nabla u|^2 dx \right) \right] \right] dx + \\ &+ \frac{\sqrt{2}}{3\varepsilon_2^2} \left[m_1^{\frac{3}{2}} \left(\int_{\Omega} |\Delta v|^2 dx \right)^{\frac{3}{2}} + m_2^{\frac{3}{2}} \left[\frac{1}{4\varepsilon_4^3} \left(\int_{\Omega} |\Delta v|^2 dx \right)^3 + \frac{3\varepsilon_4}{4} \left(\int_{\Omega} |\nabla(\Delta v)|^2 dx \right) \right] \right] dx, \end{aligned} \quad (2.46)$$

by using (2.46) in (2.37), we obtain

$$\begin{aligned} W'(t) &\leq \alpha' \int_{\Omega} u^2 dx + \left[-2\alpha + \frac{1}{\sqrt{2}} m_2^{\frac{3}{2}} k_1 \alpha \varepsilon_2 \varepsilon_3 + \frac{k_4 \beta}{\varepsilon_1} \right] \int_{\Omega} |\nabla u|^2 dx \\ &+ \left[k_4 \varepsilon_1 \beta - 2k_2 \beta + \sqrt{2} \alpha k_1 m_2^{\frac{3}{2}} \frac{\varepsilon_4}{4\varepsilon_2^2} \right] \int_{\Omega} |\nabla \Delta v|^2 dx \\ &+ \frac{2\sqrt{2}}{3} \alpha k_1 \varepsilon_2 \left[m_1^{\frac{3}{2}} \left(\int_{\Omega} u^2 dx \right)^{\frac{3}{2}} + \frac{m_2^{\frac{3}{2}}}{4\varepsilon_3^3} \left(\int_{\Omega} u^2 dx \right)^3 \right] \\ &+ \frac{\sqrt{2}}{3\varepsilon_2^2} \alpha k_1 \left[m_1^{\frac{3}{2}} \left(\int_{\Omega} (\Delta v)^2 dx \right)^{\frac{3}{2}} + \frac{m_2^{\frac{3}{2}}}{4\varepsilon_4^3} \left(\int_{\Omega} (\Delta v)^2 dx \right)^3 \right] \\ &+ (\beta' - 2k_3 \beta) \int_{\Omega} (\Delta v)^2 dx. \end{aligned} \quad (2.47)$$

Now we choose $\alpha(t)$ and $\beta(t)$ in (2.47) as

$$\alpha(t) = \frac{k_4^2 \beta}{k_2}, \quad \beta(t) = e^{2K_3(t)}, \quad \text{with } K_3(t) = \int_0^t k_3(s) ds \quad (2.48)$$

and the arbitrary functions ε_i ($for i = 1, \dots, 4$) as

$$\varepsilon_1(t) = \frac{k_2}{k_4}, \quad \varepsilon_2 = 1, \quad \varepsilon_3(t) = \frac{\sqrt{2}}{k_1 m_2^{\frac{3}{2}}}, \quad \varepsilon_4(t) = \frac{2\sqrt{2} k_2^2}{k_1 k_4^2 m_2^{\frac{3}{2}}} \quad (2.49)$$

By using these values, the coefficients of $\int_{\Omega} |\nabla u|^2 dx$ and $\int_{\Omega} |\nabla \Delta v|^2 dx$ in (2.47) vanish. Moreover

$$\alpha' = \frac{\beta k_4^2}{k_2} \left(\frac{2k_4'}{k_4} - \frac{k_2'}{k_2} + 2k_3 \right) \leq 0,$$

from hypothesis (2.35). In these circumstances we neglect in (2.47) the non negative terms and drop the terms whose coefficients are zero due to the choice of $\varepsilon_i(t)$ and $\alpha(t)$ and $\beta(t)$. By using the inequality $a^\gamma + b^\gamma \leq (a+b)^\gamma$, valid for $\gamma > 1$ and a and b non negative, at the end we obtain

$$W'(t) \leq A(t)W^{\frac{3}{2}}(t) + B(t)W^3(t), \quad (2.50)$$

where

$$\begin{cases} A = A(t) = \frac{\sqrt{2} m_1^{\frac{3}{2}} \alpha k_1}{3} = \max_{t \in [0, t^*]} \left(\frac{2\varepsilon_2}{\alpha^{\frac{3}{2}}}, \frac{1}{\varepsilon_2^2 \beta^{\frac{3}{2}}} \right), \\ B = B(t) = \frac{\sqrt{2} m_2^{\frac{3}{2}} \alpha k_1}{12} = \max_{t \in [0, t^*]} \left(\frac{2}{\alpha^3 \varepsilon_3^3}, \frac{1}{\varepsilon_4^3} \right). \end{cases}$$

CHAPTER 2. LOWER BOUNDS FOR THE BLOW-UP TIME IN A MODEL OF CHEMOTAXIS:
THE TWO- AND THREE-DIMENSIONAL CASES

With the aim to simplify (2.50), we compare the values of $W(t)$ in the time interval $[0, t^*)$ with the initial value $W_0 = W(0)$. We recall that $W(t)$ is assumed blowing up at t^* . If $W(t)$ is non decreasing in $[0, t^*)$, then $W(t) \geq W_0, \forall t \in [0, t^*)$; on the contrary, if W is non increasing, there exists a time $t_1 \in (0, t^*)$ where $W(t_1) = W_0$ and as a consequence, $W(t) \leq W_0, \forall t \in [t_1, t^*)$. This fact implies that

$$W(t)^{\frac{3}{2}} \leq W_0^{-\frac{3}{2}} W^3(t), \quad t \in [t_1, t^*), \quad (2.51)$$

Inserting (2.51) in (2.50), we obtain the desired differential inequality

$$w(t) \geq \frac{W'(t)}{W^3(t)}, \quad (2.52)$$

being

$$w(t) = W_0^{-\frac{3}{2}} A + B.$$

By integrating (2.52) between t_1 and t^* , we obtain

$$H(t^*) := \int_0^{t^*} w(\tau) d\tau \geq \int_{t_1}^{t^*} w(\tau) d\tau \geq \frac{1}{2W_0^2}. \quad (2.53)$$

This inequality provides a lower bound T for t^* with

$$T := H^{-1} \left(\frac{1}{2W_0^2} \right),$$

H^{-1} being the inverse of H ; in this way the theorem is proved. \square

Remark 3. Since k_i are strictly positive and continuous functions in $[0, t^*]$, also $w(t)$ of Theorem (2.5) is positive; H is defined in t^* and, in particular, $0 < H(t^*) = \lim_{t \rightarrow t^*} \int_0^t w(\tau) d\tau < \infty$.

Remark 4 (Another lower bound). Hypothesis (2.35) on the time depending coefficients k_i , is not strictly necessary to derive a lower bound of t^* ; in fact, from (2.48) and (2.49), (2.47) is also reduced to

$$\begin{aligned} W'(t) \leq & \frac{2\sqrt{2}}{3} \alpha k_1 \varepsilon_2 \left[m_1^{\frac{3}{2}} \left(\int_{\Omega} u^2 dx \right)^{\frac{3}{2}} + \frac{m_2^{\frac{3}{2}}}{4\varepsilon_3^3} \left(\int_{\Omega} u^2 dx \right)^3 \right] \\ & + \frac{\sqrt{2}}{3\varepsilon_2^2} \alpha k_1 \left[m_1^{\frac{3}{2}} \left(\int_{\Omega} (\Delta v)^2 dx \right)^{\frac{3}{2}} + \frac{m_2^{\frac{3}{2}}}{4\varepsilon_4^3} \left(\int_{\Omega} (\Delta v)^2 dx \right)^3 \right] \\ & + \alpha' \int_{\Omega} u^2 dx + \beta' \int_{\Omega} (\Delta v)^2 dx. \end{aligned} \quad (2.54)$$

where we have neglected the negative term $-2k_3\beta \int_{\Omega} (\Delta v)^2 dx$. This implies

$$W'(t) \leq AW^{\frac{3}{2}}(t) + BW^3(t) + CW(t),$$

where A and B have been previously computed and C is

$$C = C(t) = \max_{t \in [0, t^*]} \left(\frac{\alpha'}{\alpha}, \frac{\beta'}{\beta} \right),$$

α and β given by (2.48). Therefore, following the same reasoning of Theorem 2.5, if this function

$$\tilde{w}(t) = W_0^{-\frac{3}{2}} A + B + CW_0^{-2},$$

CHAPTER 2. LOWER BOUNDS FOR THE BLOW-UP TIME IN A MODEL OF CHEMOTAXIS:
THE TWO- AND THREE-DIMENSIONAL CASES

is considered, this inequality

$$\tilde{H}(t^*) := \int_0^{t^*} \tilde{w}(\tau) d\tau \geq \int_{t_1}^{t^*} \tilde{w}(\tau) d\tau \geq \frac{1}{2W_0^2},$$

provides another lower bound for t^* , given by

$$\tilde{T} = \tilde{H}^{-1}\left(\frac{1}{2W_0^2}\right).$$

Of course, since $\tilde{w}(t) \geq w(t)$, $\tilde{T} \leq T$, so that not considering hypothesis (2.35) returns a less accurate estimate of t^* than that given by (2.36).

As expected, we also have the bi-dimensional version of the previous theorem:

Theorem 2.6. *Let (u, v) be a classical solution of (2.32). Assume D a bounded domain in \mathbb{R}^3 , with the origin inside, star-shaped and convex in two orthogonal directions. Let W defined in (2.33) and (u, v) becomes unbounded at some time t^* in W -measure (2.34). Moreover assume that the coefficients k_i (for $i = 1, 2, 3, 4$) satisfy the following relation*

$$\frac{2k_4'}{k_4} - \frac{k_2'}{k_2} + 2k_3 \leq 0, \quad (2.55)$$

and let be

$$\begin{cases} \beta(t) = \exp^{2K_3(t)}, \text{ with } K_3(t) = \int_0^t k_3(s) d\mathbf{x}, \\ \alpha(t) = \frac{k_4^2}{k_2} \beta \end{cases}$$

Then

$$t^* \geq \bar{H}^{-1}\left(\frac{1}{2W(0)^2}\right), \quad (2.56)$$

with \bar{H}^{-1} the inverse function of $\bar{H}(t) := \int_0^t \bar{\omega}(\tau)$, $\bar{\omega}(\tau)$ being a positive function depending only on the data.

Proof. If problem (2.32) is considered in a convex domain $D \subset \mathbb{R}^2$, this lower bound for t^* can be obtained:

$$t^* \geq \bar{H}^{-1}\left(\frac{1}{W_0}\right), \quad (2.57)$$

where \bar{H}^{-1} is the inverse of

$$\bar{H}(t^*) := \int_0^{t^*} \bar{w}(\tau) d\tau,$$

$\bar{w}(\tau)$ being a positive function depending only on the data.

In fact, by means of a similar previously used technique can be replaced by

$$\int_{\Omega} u^3 d\mathbf{x} \leq \frac{\sqrt{2}}{3} m_1 \left(\int_{\Omega} u^2 d\mathbf{x} \right)^{\frac{3}{2}} + \frac{\sqrt{2}}{2} m_2 \int_{\Omega} u^2 d\mathbf{x} \left(\int_{\Omega} |\nabla u|^2 d\mathbf{x} \right)^{\frac{1}{2}},$$

and

$$\int_{\Omega} |\Delta v|^3 d\mathbf{x} \leq \frac{\sqrt{2}}{3} m_1 \left(\int_{\Omega} |\Delta v|^2 d\mathbf{x} \right)^{\frac{3}{2}} + \frac{\sqrt{2}}{2} m_2 \int_{\Omega} |\Delta v|^2 d\mathbf{x} \left(\int_{\Omega} |\nabla(\Delta v)|^2 d\mathbf{x} \right)^{\frac{1}{2}},$$

m_1 and m_2 in Lemma A.3.

Finally, by arranging the proof of Theorem 2.5, estimate (2.57) can be checked. \square

Chapter 3

Numerical resolution method for the Keller–Segel system

There exist numerous papers devoted to the quantitative analysis of blowing up solutions of problems defined on bounded or unbounded domains (see [1] and [3]). In this sense, starting from the natural weak formulation associated to problem (2.3), we propose an algorithm based on a mixed Finite Element Method in space and Euler Method in time (see [25]) capable of numerically solving such system. This resolution approach is implemented in the 2D case to analyze the behaviors of the norm of the maximum of some blowing up solutions of (2.3) with different domains and (2.32), where the k_i coefficients are even time-dependent regular functions.

We wish to remark that in Appendix §B we include some known and classical concepts often employed in numerical analysis to simulate models formulated by means of partial differential equations.

3.1 Semi-discretization in space

If a mesh of $\Omega \subset \mathbb{R}^n$ ($n = 2, 3$) is fixed and N represents the total number of nodes of Ω , let (U, V) be the numerical approximation of the solution (u, v) of (2.3) and (2.32): therefore, by separating variables

$$\begin{cases} U(\mathbf{x}, t) = \sum_{i=1}^N u^i(t)\phi^i(x), \\ V(\mathbf{x}, t) = \sum_{i=1}^N v^i(t)\phi^i(x), \end{cases} \quad (3.1)$$

where $\phi^i(\mathbf{x})$ is the standard quadratic basis function at the vertex \mathbf{x}^i , for $i = 1, \dots, N$.

Thanks to the divergence theorem and the homogeneous boundary conditions of the Keller-Segel system, by multiplying its first two equations by a generic test function ϕ^j , the following variational form in space is achieved:

$$\begin{cases} \int_{\Omega} U_t \phi^j dx + \int_{\Omega} \nabla U \cdot \nabla \phi^j = k_1 \int_{\Omega} (U \nabla V) \cdot \nabla \phi^j, \\ \int_{\Omega} V_t \phi^j dx + k_2 \int_{\Omega} \nabla V \cdot \nabla \phi^j = k_4 \int_{\Omega} U \phi^j - k_3 \int_{\Omega} V \phi^j. \end{cases} \quad (3.2)$$

If $(\cdot; \cdot)$ denotes the usual L^2 inner product

$$\begin{cases} (U_t, \phi^j) + (\nabla U, \nabla \phi^j) = k_1 (U \nabla V, \nabla \phi^j), \\ (V_t, \phi^j) + k_2 (\nabla V, \nabla \phi^j) = k_4 (U, \phi^j) - k_3 (V, \phi^j). \end{cases} \quad (3.3)$$

Semi-discretization in time

To compute the time evolutions of both coefficients u^i and v^i appearing in 3.1, let $\Delta t = t_{m+1} - t_m$ be a given time step, with $m = 0, 1, 2, \dots (t_0 = 0)$, and (U_m, V_m) the approximation of $(U(\mathbf{x}, t), V(\mathbf{x}, t))$ at time t_m . By applying an implicit Euler finite difference approximation to system 3.3, it is seen that

$$\begin{cases} \frac{1}{\Delta t}(U_{m+1} - U_m, \phi^j) + (\nabla U_{m+1}, \nabla \phi^j) = k_1(U_m \nabla V_m, \nabla \phi^j), \\ \frac{1}{\Delta t}(V_{m+1} - V_m, \phi^j) + k_2(\nabla V_{m+1}, \nabla \phi^j) = k_4(U_m, \phi^j) - k_3(V_m, \phi^j), \end{cases}$$

i.e., taking into account (3.1),

$$\mathbf{M} \frac{\mathbf{u}_{m+1} - \mathbf{u}_m}{\Delta t} + \mathbf{K} \mathbf{u}_{m+1} = k_1 \mathbf{F}(\mathbf{u}_m, \mathbf{v}_m),$$

and

$$\mathbf{M} \frac{\mathbf{v}_{m+1} - \mathbf{v}_m}{\Delta t} + k_2 \mathbf{K} \mathbf{v}_{m+1} = k_4 \mathbf{M} \mathbf{u}_m - k_3 \mathbf{M} \mathbf{v}_m,$$

with $\mathbf{M} \in \mathbb{R}^{N \times N}$ (mass matrix), $\mathbf{K} \in \mathbb{R}^{N \times N}$ (stiffness matrix) and $\mathbf{F}(\mathbf{u}_m, \mathbf{v}_m) \in \mathbb{R}^N$ such that

$$\begin{cases} \mathbf{M}_{ij} = \int_{\Omega} \phi^i(\mathbf{x}) \phi^j(\mathbf{x}) d\mathbf{x}, \\ \mathbf{K}_{ij} = \int_{\Omega} \nabla \phi^i(\mathbf{x}) \cdot \nabla \phi^j(\mathbf{x}) d\mathbf{x}, \\ \mathbf{F}(\mathbf{u}_m, \mathbf{v}_m)_j = \int_{\Omega} \left(\sum_{p,q=1}^N u_m^p v_m^q \phi^p(\mathbf{x}) \nabla \phi^q(\mathbf{x}) \right) \cdot \nabla \phi^j(\mathbf{x}) d\mathbf{x}, \end{cases}$$

being $\mathbf{u}_m = (u_m^1, \dots, u_m^N)^T$ and $\mathbf{v}_m = (v_m^1, \dots, v_m^N)^T$, where T indicates the transposition operator. Under these circumstances, (u_m^i, v_m^i) represents the approximation of the solution (u, v) of problem Keller-Segel at time t_m , for $m = 0, 1, 2, \dots$, and at space point \mathbf{x}^i , for $i = 1, 2, \dots, N$.

In this way the continuous solution of the nonlinear system Keller-Segel is identified to the discrete solution of the linear system

$$\begin{cases} \mathbf{A} \mathbf{u}_{m+1} = \mathbf{b}, \\ \mathbf{B} \mathbf{v}_{m+1} = \mathbf{c}, \end{cases}$$

with

$$\begin{cases} \mathbf{A} = \frac{1}{\Delta t} \mathbf{M} + \mathbf{K}, \\ \mathbf{B} = \frac{1}{\Delta t} \mathbf{M} + k_2 \mathbf{K}, \\ \mathbf{b} = \frac{1}{\Delta t} \mathbf{M} \mathbf{u}_m + k_1 \mathbf{F}(\mathbf{u}_m, \mathbf{v}_m), \\ \mathbf{c} = \frac{1}{\Delta t} \mathbf{M} \mathbf{v}_m + k_4 \mathbf{M} \mathbf{u}_m - k_3 \mathbf{M} \mathbf{v}_m. \end{cases}$$

3.2 Numerical tests for $n = 2$

Let us dedicate to simulate some specific cases of our main system (2.3). In particular, since we want to examine more general situations, we precisely will analyze this problem

$$\begin{cases} u_t = k_0 \Delta u - k_1 \nabla \cdot (u \nabla v), \\ v_t = k_2 \Delta v - k_3 v + k_4 u, \end{cases} \quad (3.4)$$

with usual Neuman boundary conditions and initial data. Herein, moreover, k_i , $i = 0, 1, 2, 3, 4$ may be functions of the time variable t and the space variable \mathbf{x} .

Let us consider the domain $Q = \Omega \times \mathbb{R}_0^+$, being $\Omega = [-2, 2] \times [-2, 2]$ the square with center in the origin of the axes $O(0, 0)$ and length 4. We take a uniform mesh, obtained by dividing each side of the square into 200 equal parts (i.e. 40401 vertexes and 80000 triangles). We also choose $v_0 = 0.55e^{-(x^2+y^2)}(4-x^2)^2(4-y^2)^2$ (the chemical signal at time $t_0 = 0$) and $u_0(\mathbf{x}) = 1.15e^{-(x^2+y^2)}(4-x^2)(4-y^2)^2$ (the bacteria at time $t_0 = 0$) as initial conditions and $\epsilon_0 = 10^4$ as the threshold and $\Delta t = 10^{-4}$ as the integration step.

As to the blow-up scenario, we establish this criterion to decide whether it happens or not: *let us fix the threshold* $\epsilon_0 = 10^4$ and the integer number $N = 250$. We say that u blows-up at a certain point \mathbf{x}_i of the mesh and a certain time t^j if $u(\mathbf{x}_i, t^j) > \epsilon_0$, for some $j = 1, \dots, N$. Conversely u does not blow-up and it is global.

In order to solve the below tests, we use the free software called Freefem ++, which is a robust and friendly programming language focused on solving partial differential equations using the finite element method. In particular, for the convenience of the reader, we add the entire code of a specific case in Appendix §C.

3.2.1 Tests with time and space dependent coefficients

Let us apply the numerical method previously proposed to some precise cases. In particular, once these data are set, we will solve system (3.4) in six different cases, all of these characterized by coefficients k_i which depend on time and space: the first four cases dealing with time dependent coefficients (for brevity *TDC – Test*) and the remaining two with space dependent coefficients (i.e., *SDC – Test*)

In particular we will fix the same square than above and these initial data:

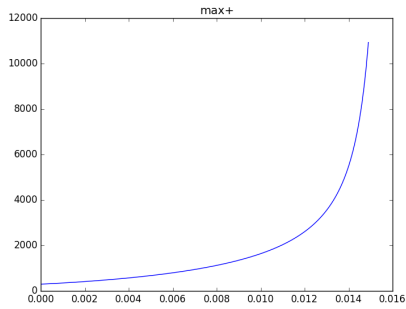
$$\begin{cases} u_0(\mathbf{x}) = 1.15e^{-(x^2+y^2)}(4-x^2)(4-y^2)^2, \\ v_0(\mathbf{x}) = 0.55e^{-(x^2+y^2)}(4-x^2)^2(4-y^2)^2. \end{cases}$$

star with three tests, where we will study system (3.4) when k_0 and k_2 vary over time and $k_1 = 0.2$, $k_3 = 0.1$ and $k_4 = 1$. In the fourth test we study the case in which k_0 and k_2 vary over time but unlike previous ones, the value k_1 is 0.1. In the last two tests, we will study, the case in which k_0 varies in space. In the first test we choose $k_0 = x^2 + y^2$ and in the second test we choose $k_0 = 3xy$.

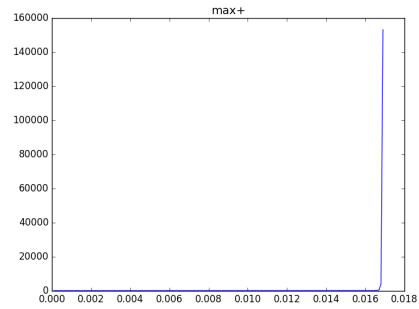
Time dependent coefficient case

- Test *TDC – Test*₁: $k_0 = t^2, k_1 = 0.2, k_2 = k_4 = 1$ and $k_3 = 0.1$. The graphical result is shown in Figures 3.1 and 3.2. We can observe that the same qualitative results are obtain if we consider these other data: $k_0 = t, k_1 = 0.2, k_2 = k_4 = 1$ and $k_3 = 0.1$.
- Test *TDC – Test*₂: $k_0 = 1, k_1 = 0.2, k_2 = t^2, k_3 = 0.1$ and $k_4 = 1$. The graphical result is shown in Figures 3.3 and 3.4. We can observe that the same qualitative results are obtain if we consider these other data: $k_0 = 1, k_1 = 0.2, k_2 = t, k_3 = 0.1$ and $k_4 = 1$.
- Test *TDC – Test*₃: $k_0 = t, k_1 = 0.2, k_2 = t^2, k_3 = 0.1, k_4 = 1$. The graphical result is shown in Figures 3.5 and 3.6. We can observe that the same qualitative results are obtain if we consider these other data: $k_0 = t^2, k_1 = 0.2, k_2 = t, k_3 = 0.1$ and $k_4 = 1$, and $k_0 = t, k_1 = 0.2, k_2 = t, k_3 = 0.1$ and $k_4 = 1$.
- Test *TDC – Test*₄: $k_0 = t, k_1 = 0.1, k_2 = t, k_3 = 0.1$ and $k_4 = 1$. The graphical result is shown in Figures 3.7 and 3.8. We can observe that the same qualitative results are obtain if we consider these other data: $k_0 = t^2, k_1 = 0.1, k_2 = t, k_3 = 0.1$ and $k_4 = 1$ and $k_0 = t, k_1 = 0.1, k_2 = t^2, k_3 = 0.1$ and $k_4 = 1$. It is worth to observe that replacing $k_1 = 0.2$ with $k_1 = 0.1$, the instability does not appear. Subsequently, from this observation and the analysis of the presented tests, we could conclude that such a singular behavior may be related to the fact that, unlike the previous

cases, both the coefficients of the diffusive terms associated to u and v are herein time-dependent and the largeness of k_1 .

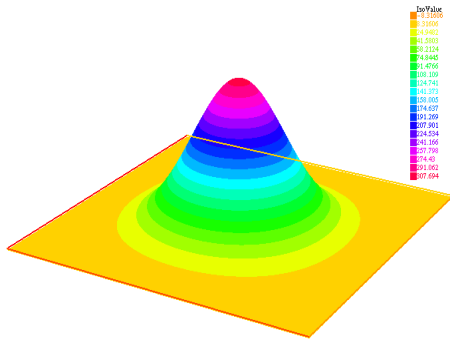


(a) Evolution of $\max_{\mathbf{x} \in \Omega} |u(\mathbf{x}, t)|$

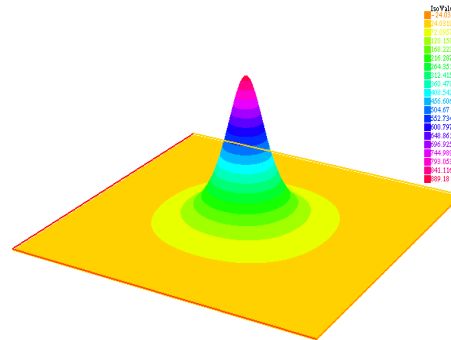


(b) Evolution of $\max_{\mathbf{x} \in \Omega} |v(\mathbf{x}, t)|$

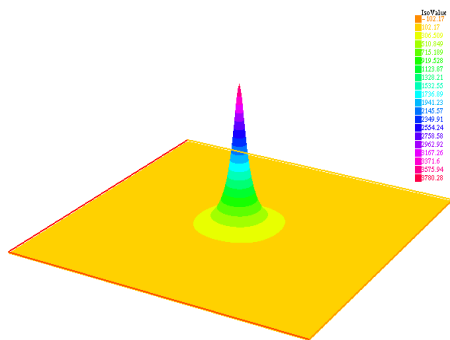
Figure 3.1: Test $TDC - Test_1$: Analysis of the behaviors of $u(\mathbf{x}, t)$ and $v(\mathbf{x}, t)$



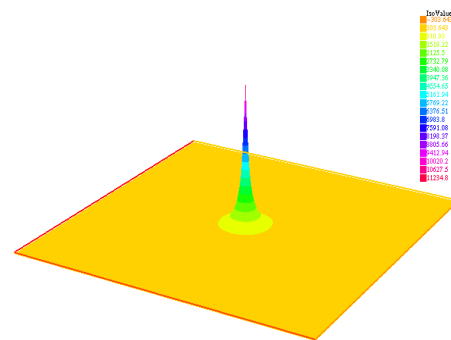
(a) Solution u at time $t \approx 0.0003$; $\max u = u(O) \approx 309.574$. Note that the red color (maximum value) is 307.694 and the orange color (minimum value) is 8.31606.



(b) Solution u at time $t \approx 0.0067$; $\max u = u(O) \approx 895.039$. Note that the red color (maximum value) is 889.18 and the orange color (minimum value) is 24.0319.

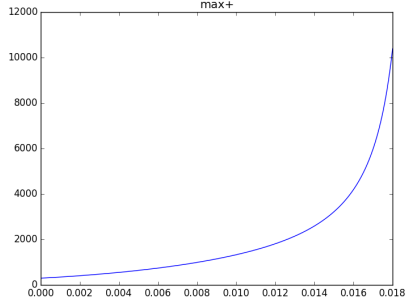


(c) Solution u at time $t \approx 0.0133$; $\max u = u(O) \approx 3968.85$. Note that the red color (maximum value) is 3780.28 and the orange color (minimum value) is 102.17.

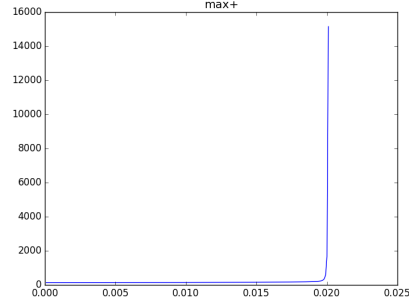


(d) Solution u at time $t \approx 0.0149$; $\max u = u(O) \approx 10931.2$. Note that the red color (maximum value) is 11234.8 and the orange color (minimum value) is 303.643.

Figure 3.2: Test $TDC - Test_1$: numerical solution. Evolution of u and its graphical representation: with t increasing the value of u at O increases. According to the blow-up criterion given at page 21, u blows-up at $t \approx 0.0149$.

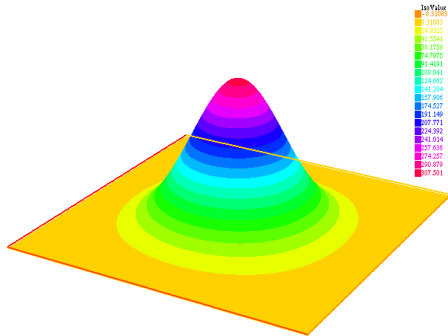


(a) Evolution of $\max_{\mathbf{x} \in \Omega} |u(\mathbf{x}, t)|$

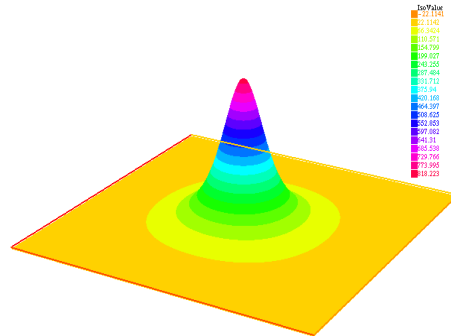


(b) Evolution of $\max_{\mathbf{x} \in \Omega} |v(\mathbf{x}, t)|$

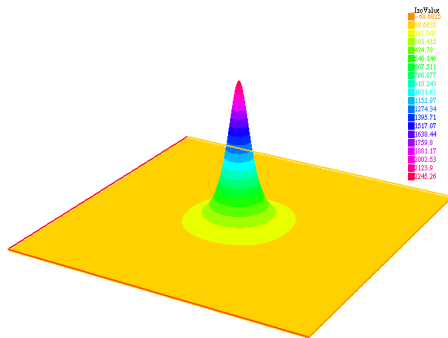
Figure 3.3: Test $TDC - Test_2$: Analysis of the behaviors of $u(\mathbf{x}, t)$ and $v(\mathbf{x}, t)$



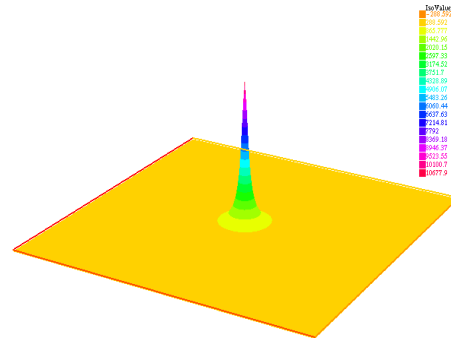
(a) Solution u at time $t \approx 0.0003$; $\max u = u(O) \approx 308.981$. Note that the red color (maximum value) is 307.501 and the orange color (minimum value) is 8.31083.



(b) Solution u at time $t \approx 0.0067$; $\max u = u(O) \approx 819.652$. Note that the red color (maximum value) is 818.223 and the orange color (minimum value) is 22.1142.



(c) Solution u at time $t \approx 0.0133$; $\max u = u(O) \approx 2265.37$. Note that the red color (maximum value) is 2245.26 and the orange color (minimum value) is 60.6832.



(d) Solution u at time $t \approx 0.018$; $\max u = u(O) \approx 10389.3$. Note that the red color (maximum value) is 10677.9 and the orange color (minimum value) is 288.592.

Figure 3.4: Test $TDC - Test_2$: numerical solution. Evolution of u and its graphical representation: with t increasing the value of u at O increases. According to the blow-up criterion given at page 21, u blows-up at $t \approx 0.018$.

Remark 5. It is worth to mention that the phenomenon detected in Figures 3.6 and 3.8, precisely corresponding to the appearance of certain instabilities, can be justified by different motivations. Indeed, if from the one hand once could imagine that it is tied to some numerical problem (for instance connected

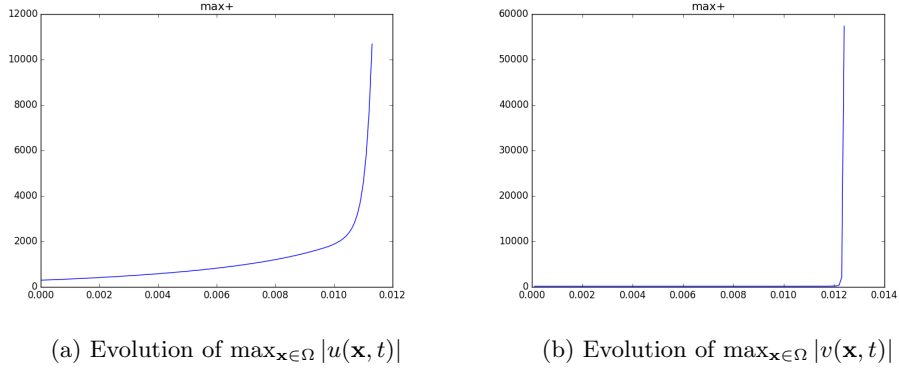


Figure 3.5: Test $TDC - Test_3$: Analysis of the behaviors of $u(\mathbf{x}, t)$ and $v(\mathbf{x}, t)$

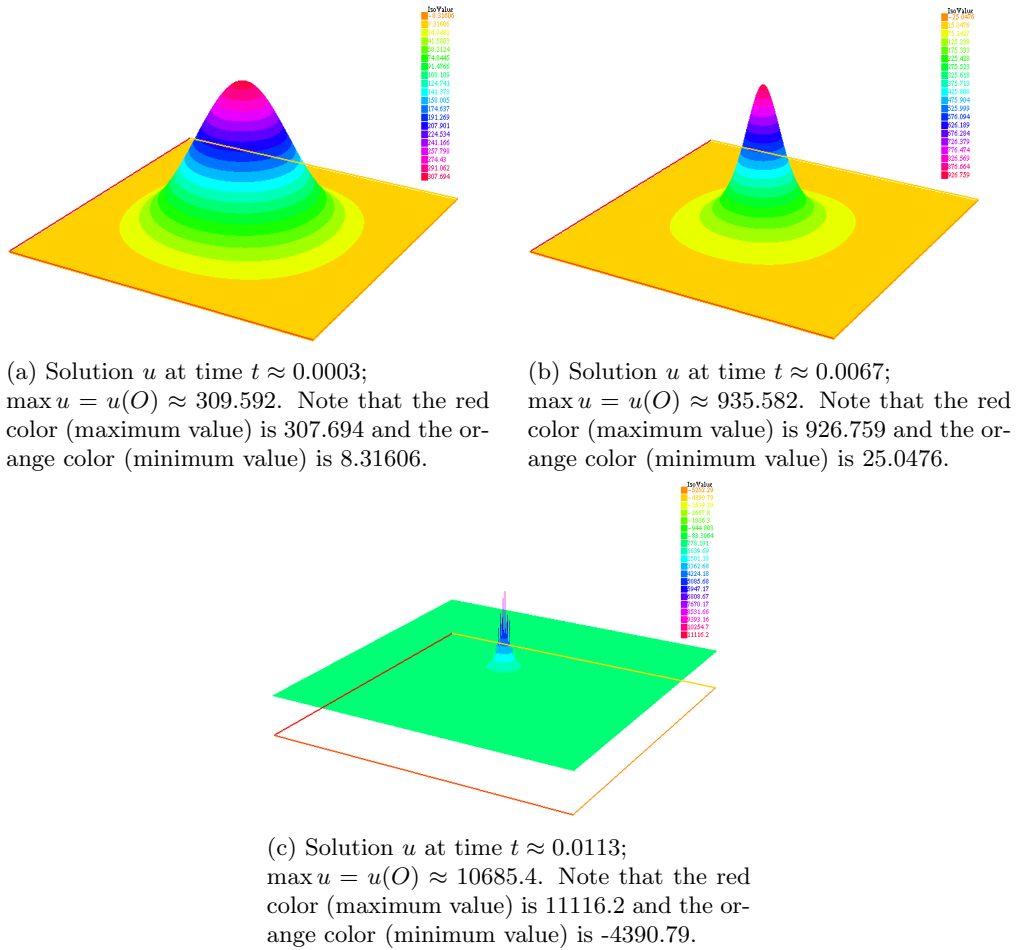
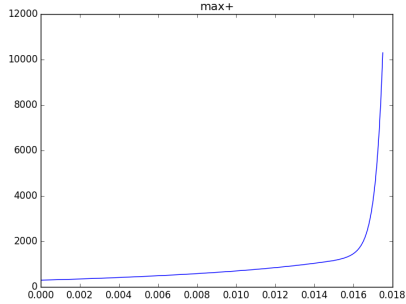


Figure 3.6: Test $TDC - Test_3$: numerical solution. Evolution of u and its graphical representation: with t increasing the value of u presents instability.

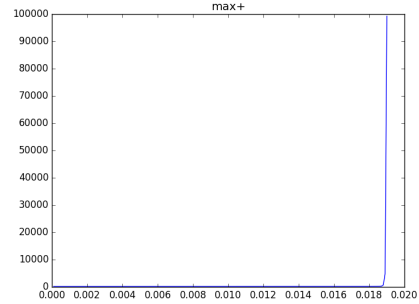
to the size of the mesh or of the time interval), on the other it is also reasonable that such “irregularity” might be associated to the model; in fact, this biological phenomena are very sensitive to small perturbations of the data.

Further, this same instability (possibly also tied to some numerical issue) makes that, in a very

CHAPTER 3. NUMERICAL RESOLUTION METHOD FOR THE KELLER–SEGEL SYSTEM

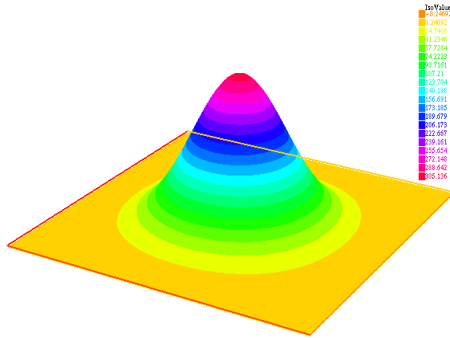


(a) Evolution of $\max_{\mathbf{x} \in \Omega} |u(\mathbf{x}, t)|$

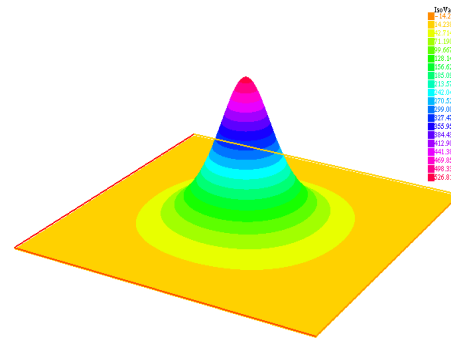


(b) Evolution of $\max_{\mathbf{x} \in \Omega} |v(\mathbf{x}, t)|$

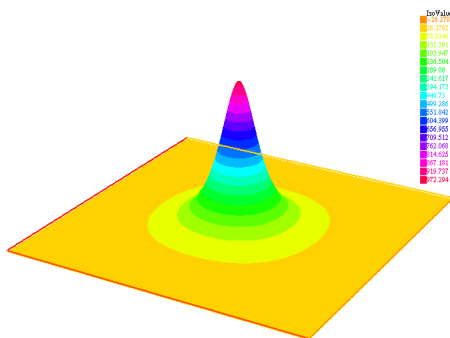
Figure 3.7: Test $TDC - Test_4$: Analysis of the behaviors of $u(\mathbf{x}, t)$ and $v(\mathbf{x}, t)$



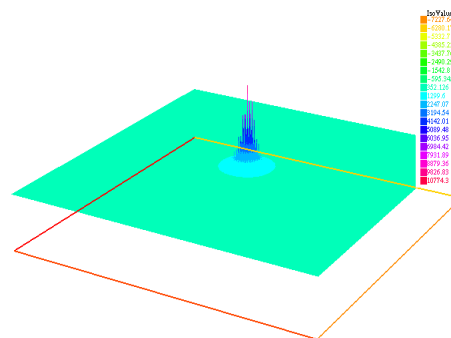
(a) Solution u at time $t \approx 0.0003$; $\max u = u(O) \approx 301.932$. Note that the red color (maximum value) is 305.136 and the orange color (minimum value) is 8.24692.



(b) Solution u at time $t \approx 0.0067$; $\max u = u(O) \approx 521.607$. Note that the red color (maximum value) is 526.811 and the orange color (minimum value) is 14.2381.



(c) Solution u at time $t \approx 0.0133$; $\max u = u(O) \approx 965.639$. Note that the red color (maximum value) is 972.294 and the orange color (minimum value) is 26.2782.



(d) Solution u at time $t \approx 0.0175$; $\max u = u(O) \approx 10300.6$. Note that the red color (maximum value) is 10774.3 and the orange color (minimum value) is -6280.17.

Figure 3.8: Test $TDC - Test_4$: numerical solution. Evolution of u and its graphical representation: with t increasing the value of u presents instability.

unexpected way, the u -component achieve also negative values; this is of course inconsistent with the physical and mathematical problem.

Space dependent coefficient case

- Test *SDC – Test*₁: $k_0 = x^2 + y^2, k_1 = 0.2, k_2 = k_4 = 1$ and $k_3 = 0.1$. The graphical result is shown in Figures 3.9 and 3.10
- Test *SDC – Test*₂: $k_0 = 3xy, k_1 = 0.2, k_2 = k_4 = 1$ and $k_3 = 0.1$. The graphical result is shown in Figures 3.11 and 3.12

3.2.2 Tests with constant coefficients

Under the same hypotheses made in §3.2.1, precisely on the domain, mesh, initial functions, threshold ε_0 and integration step, let us analyze solutions of system (3.4) with k_1 varying, fixing the other data as

$$\begin{cases} k_0 = 1, k_2 = k_4 = 1, k_3 = 0.1, \\ u_0(\mathbf{x}) = 1.15^{-(x^2+y^2)}(4-x^2)(4-y^2)^2, \quad v_0(\mathbf{x}) = 0.55e^{-(x^2+y^2)}(4-x^2)^2(4-y^2)^2. \end{cases}$$

As before, in order to select and distinguish properly our cases we identify a single test with *ConstCoef – Test*

- Test *ConstCoef – Test*₁: $k_0 = 1, k_1 = 0.01, k_2 = k_4 = 1$ and $k_3 = 0.1$. The graphical result is shown in Figures 3.13 and 3.14
- Test *ConstCoef – Test*₂: $k_0 = 1, k_1 = 0.1, k_2 = k_4 = 1$ and $k_3 = 0.1$. The graphical result is shown in Figures 3.15 and 3.16
- Test *ConstCoef – Test*₃: $k_0 = 1, k_1 = 0.2, k_2 = k_4 = 1$ and $k_3 = 0.1$. The graphical result is shown in Figures 3.17 and 3.18

Remark 6. From the three numerical tests *ConstCoef – Test*, it is clear that as expected the blow-up scenario is tied to the largeness of the cross-diffusive term k_1 , once of course the other parameters are fixed and maintained throughout the tests.

Tests with k_i constants and different initial functions

Now we analyze the solutions of the system (3.4) in case we have k_i constants and the same hypotheses made in §3.2.1 regarding domain, mesh, threshold ε_0 and integration step. To be precise we set

$$\begin{cases} k_0 = 1, k_1 = 0.2, k_2 = k_4 = 1, k_3 = 0.1, \\ v_0(\mathbf{x}) = 0.55e^{-(x^2+y^2)}(4-x^2)^2(4-y^2)^2, \end{cases}$$

and change initial functions u_0 .

- Test *InitialFunc – Test*₁, for $u_0(\mathbf{x}) = 1.15^{-(x^2+y^2)}(4-x^2)(4-y^2)^2$. The graphical result is shown in Figures 3.19 and 3.20
- Test *InitialFunc – Test*₂, for $u_0(\mathbf{x}) = 24(((x^2-4)^2 + (y^2-4)^2 + 1) - 0.05((x^2-4)^4 + (y^2-4)^4))$. The graphical result is shown in Figures 3.21 and 3.22

Remark 7. We see that in the Test *InitialFunc – Test*₂ the blow-up point is the center of the square despite the fact that in the second case u_0 has a minimum in such center. This is not a general rule; indeed, there are cases where the blow-up point is far from the center or more than a single blow-up point appear.

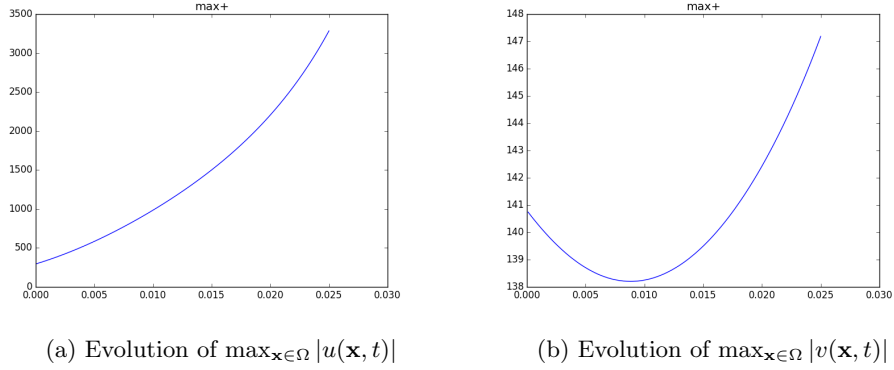


Figure 3.9: Test $SDC - Test_1$: Analysis of the behaviors of $u(\mathbf{x}, t)$ and $v(\mathbf{x}, t)$

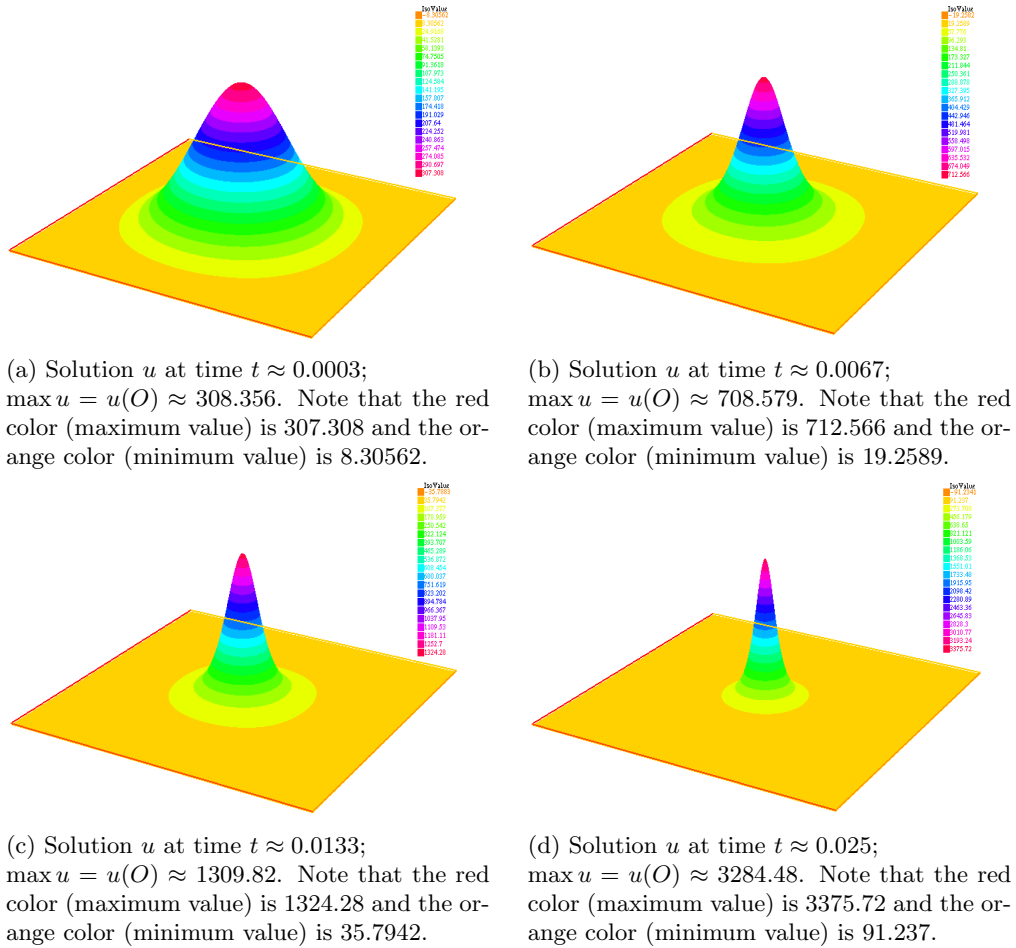


Figure 3.10: Test $SDC - Test_1$: numerical solution. Evolution of u and its graphical representation: with t increasing the value of u at O increases.

Tests with k_i constants and different domains

Now, we analyze the solutions of the system (3.4) where k_i are constants and we have the same hypotheses made in §3.2.1 regarding initial functions, mesh, threshold ε_0 and integration step, but on different

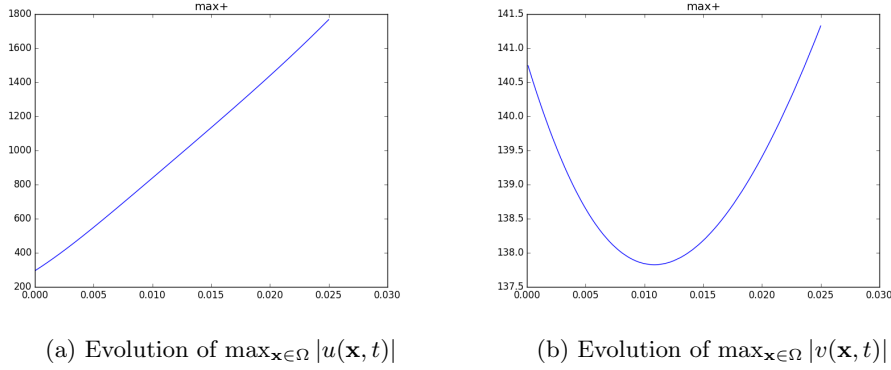


Figure 3.11: Test $SDC - Test_2$: Analysis of the behaviors of $u(\mathbf{x}, t)$ and $v(\mathbf{x}, t)$

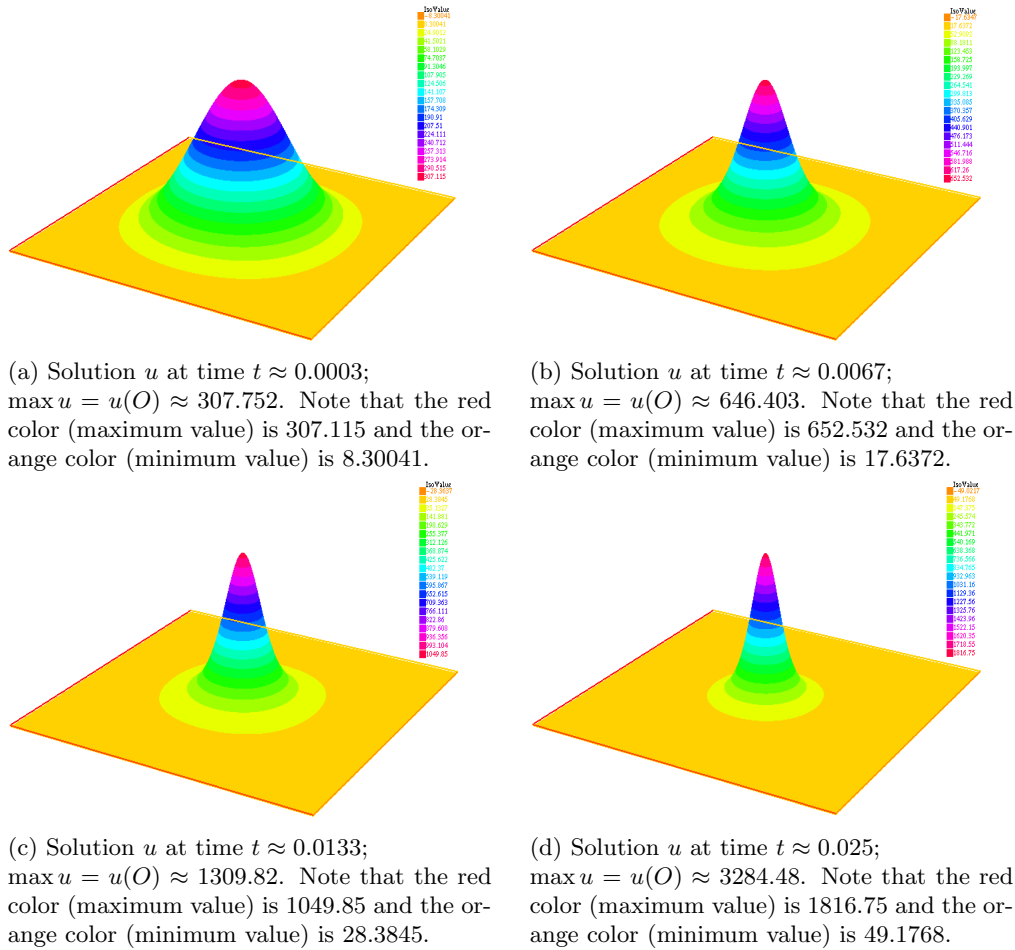


Figure 3.12: Test $SDC - Test_2$: numerical solution. Evolution of u and its graphical representation: with t increasing the value of u at O increases.

domains. We, again, set:

$$\begin{cases} k_0 = 1, k_1 = 0.2, k_2 = k_4 = 1, k_3 = 0.1, \\ u_0(\mathbf{x}) = 1.15^{-(x^2+y^2)}(4-x^2)(4-y^2)^2, \quad v_0(\mathbf{x}) = 0.55e^{-(x^2+y^2)}(4-x^2)^2(4-y^2)^2. \end{cases}$$

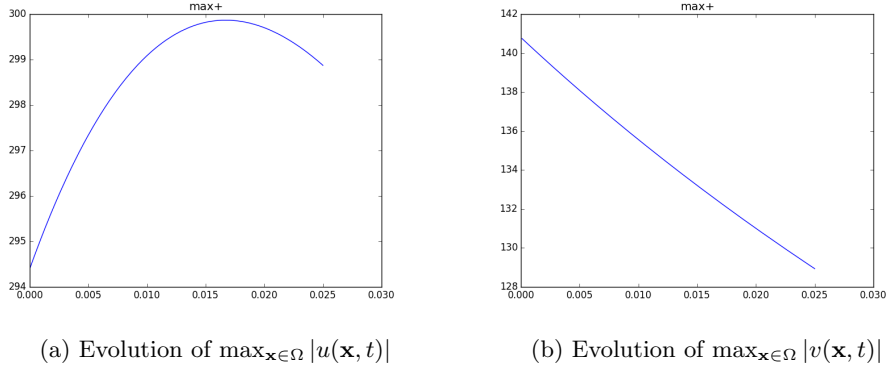


Figure 3.13: Test *CCT – Test₁*: Analysis of the behaviors of $u(\mathbf{x}, t)$ and $v(\mathbf{x}, t)$

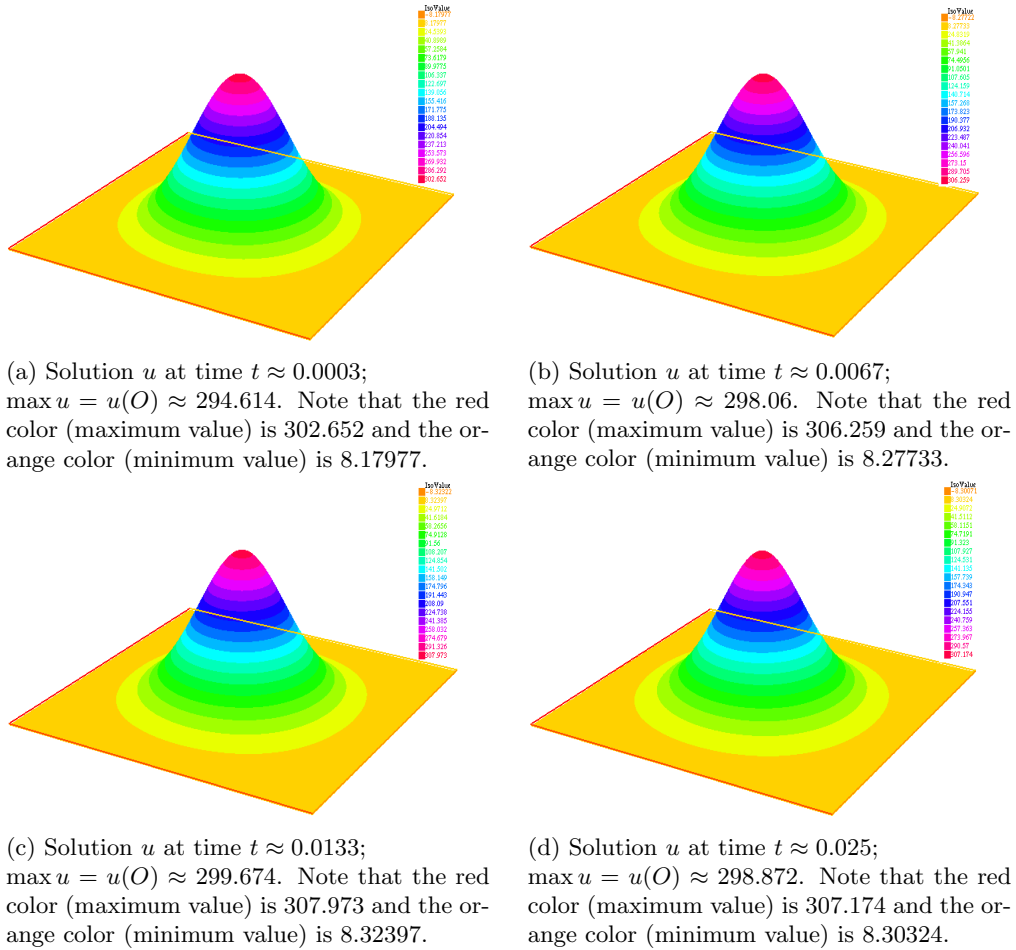
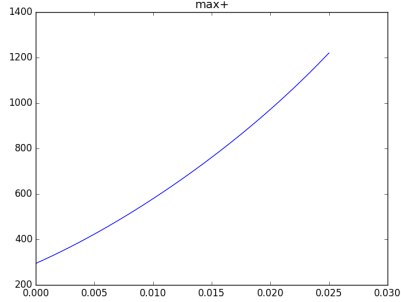
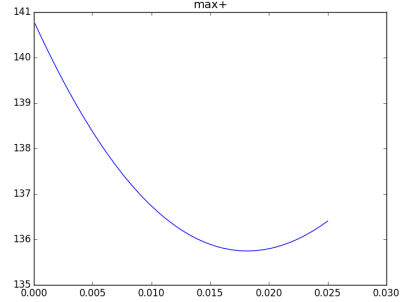


Figure 3.14: Test *CCT – Test₁*: numerical solution. Evolution of u and its graphical representation: with t increasing the value of u at O increases.

- Test *DiffDom – Test₁*: Let us consider the domain $Q = \Omega \times \mathbb{R}_0^+$, being Ω the triangle of vertices $(0, 0)$, $(1, 0)$, $(0, 1)$. The graphical result is shown in Figures 3.23 and 3.24
- Test *DiffDom – Test₂*: Let us consider the domain $Q = \Omega \times \mathbb{R}_0^+$, being Ω the ellipsoidal crown.

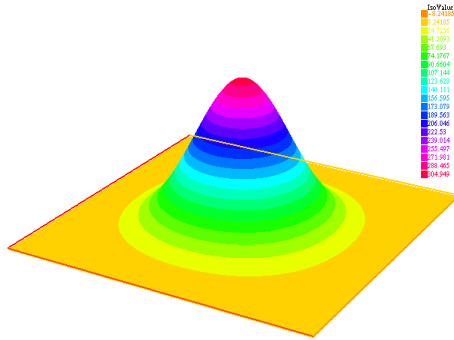


(a) Evolution of $\max_{\mathbf{x} \in \Omega} |u(\mathbf{x}, t)|$

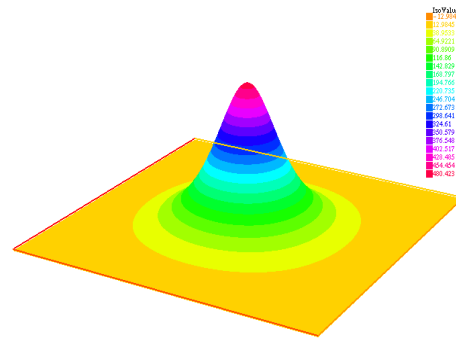


(b) Evolution of $\max_{\mathbf{x} \in \Omega} |v(\mathbf{x}, t)|$

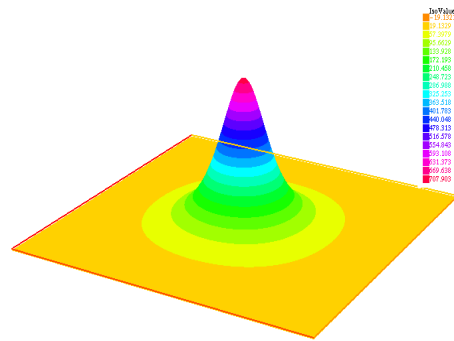
Figure 3.15: Test $CCT - Test_2$: Analysis of the behaviors of $u(\mathbf{x}, t)$ and $v(\mathbf{x}, t)$



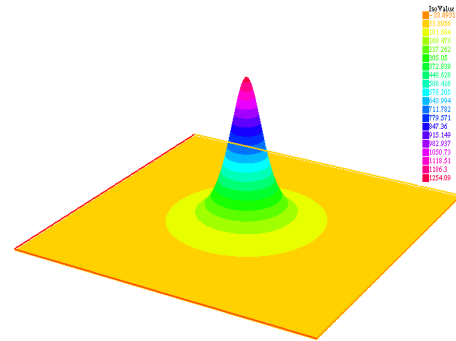
(a) Solution u at time $t \approx 0.0003$; $\max u = u(O) \approx 301.354$. Note that the red color (maximum value) is 304.949 and the orange color (minimum value) is 8.24185.



(b) Solution u at time $t \approx 0.0067$; $\max u = u(O) \approx 473.484$. Note that the red color (maximum value) is 480.423 and the orange color (minimum value) is 12.9845.



(c) Solution u at time $t \approx 0.0133$; $\max u = u(O) \approx 696.19$. Note that the red color (maximum value) is 307.694 and the orange color (minimum value) is 707.903.



(d) Solution u at time $t \approx 0.025$; $\max u = u(O) \approx 1220.2$. Note that the red color (maximum value) is 307.694 and the orange color (minimum value) is 1254.09.

Figure 3.16: Test $CCT - Test_2$: numerical solution. Evolution of u and its graphical representation: with t increasing the value of u at O increases.

$x = 1.5 \cos(t)$, $y = \sin(t)$ for $t = (2\pi, 0)$; $x = 2 \cos(t)$, $y = 2 \sin(t)$ for $t = (0, 2\pi)$. The graphical result is shown in Figures 3.25 and 3.26

Remark 8. Tests $DiffDom - Test_1$ and $DiffDom - Test_2$ show that our problem is also sensitive to

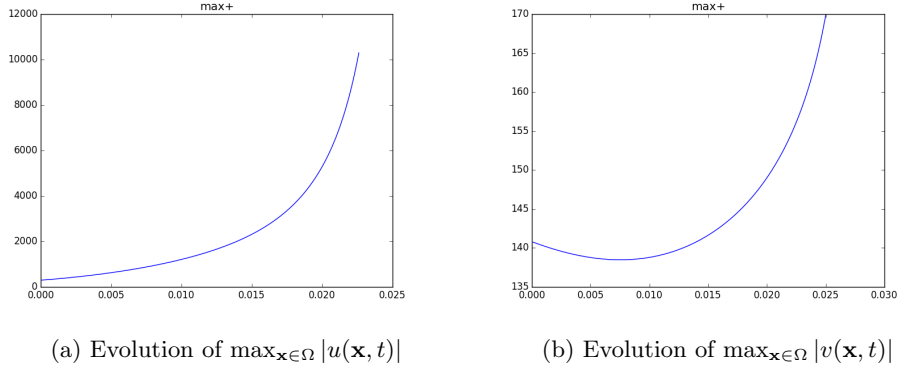


Figure 3.17: Test *CCT – Test₃*: Analysis of the behaviors of $u(\mathbf{x}, t)$ and $v(\mathbf{x}, t)$

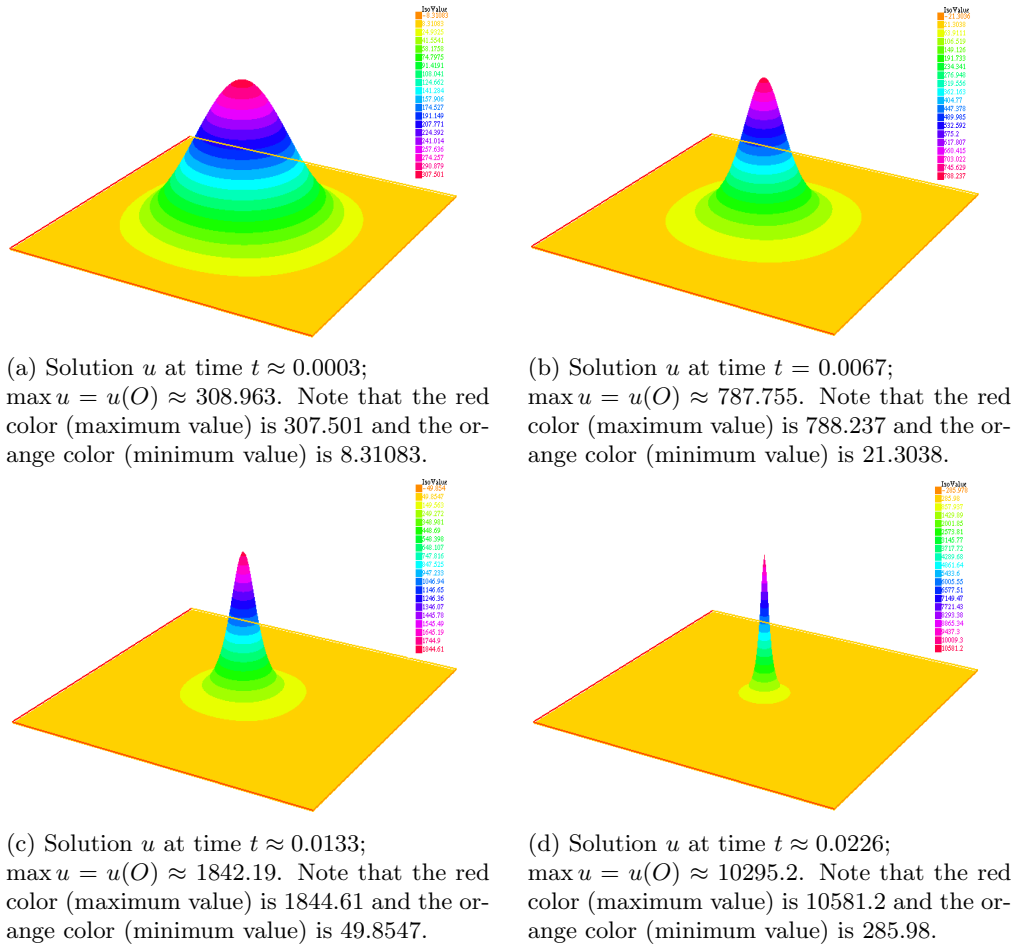


Figure 3.18: Test *CCT – Test₃*: numerical solution. Evolution of u and its graphical representation: with t increasing the value of u at O increases. According to the blow-up criterion given at page 21, u blows-up at $t \approx 0.0226$.

the domain. Indeed, fixing the parameters and the initial data we note two different behaviors of the solution when the domain is starry (L-shape) and when it is a double crown; in the first case blow-up appears, in the second it does not.

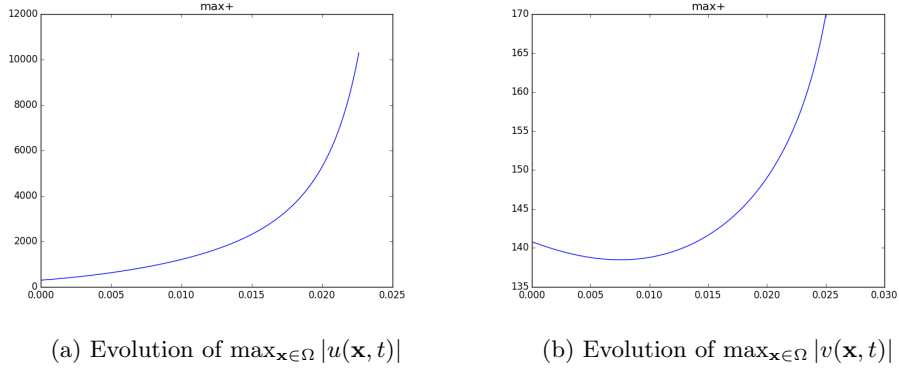


Figure 3.19: Test $IFT - Test_1$: Analysis of the behaviors of $u(\mathbf{x}, t)$ and $v(\mathbf{x}, t)$

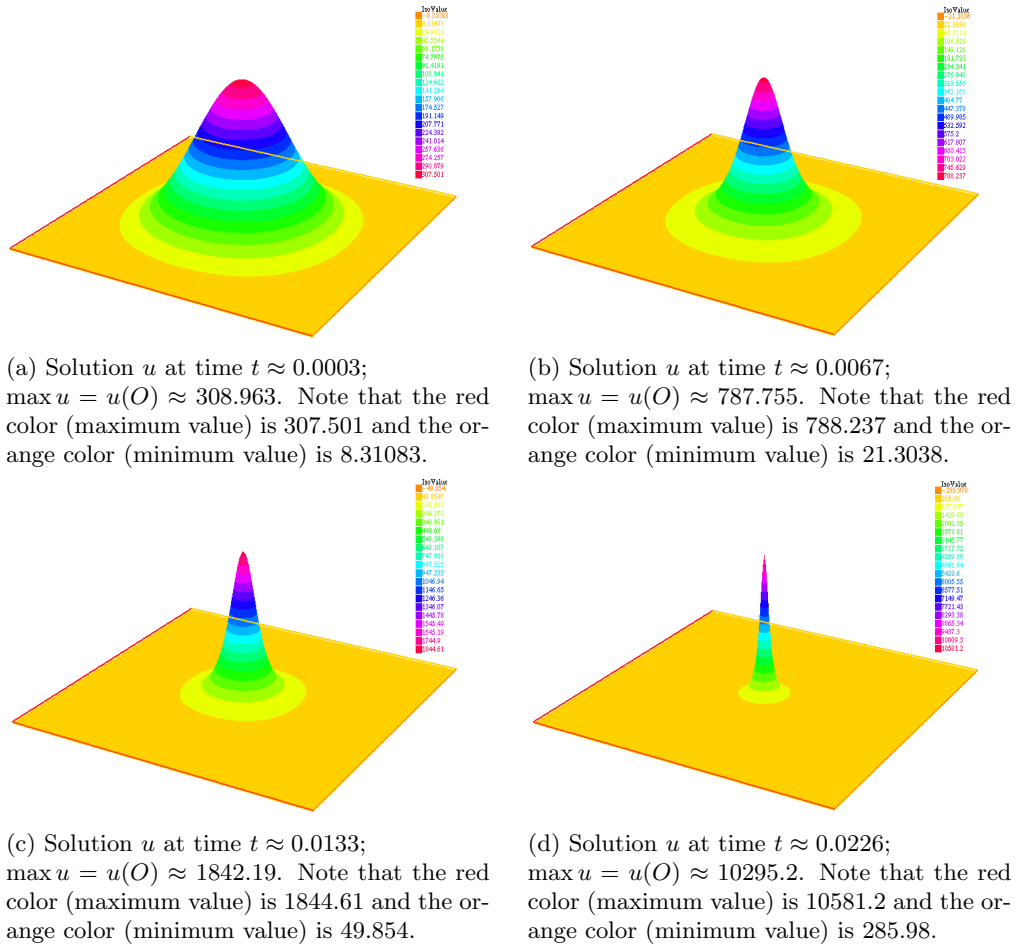


Figure 3.20: Test $IFT - Test_1$: numerical solution. Evolution of u and its graphical representation: with t increasing the value of u at O increases. According to the blow-up criterion given at page 21, u blows-up at $t \approx 0.0226$.

3.2.3 Test with negative k_1 coefficient

With the same hypotheses made in §3.2.1 regarding domain, mesh, initial functions, threshold ε_0 and integration step, now in the Figures 3.27 and 3.28 we analyze the solutions of the system (3.4) in the case

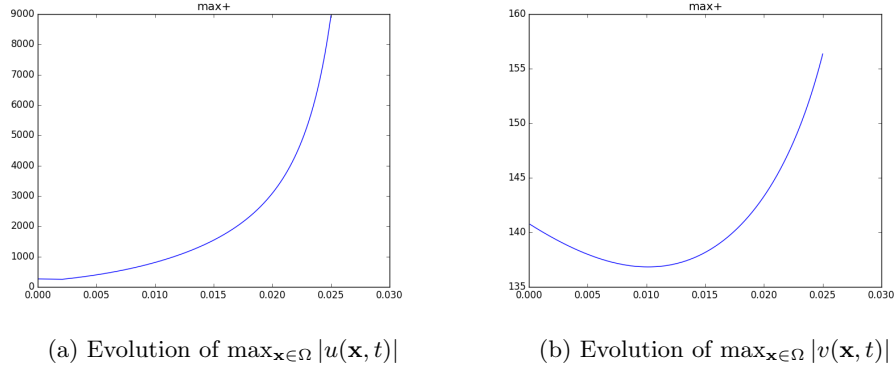


Figure 3.21: Test *IFT – Test₂*: Analysis of the behaviors of $u(\mathbf{x}, t)$ and $v(\mathbf{x}, t)$

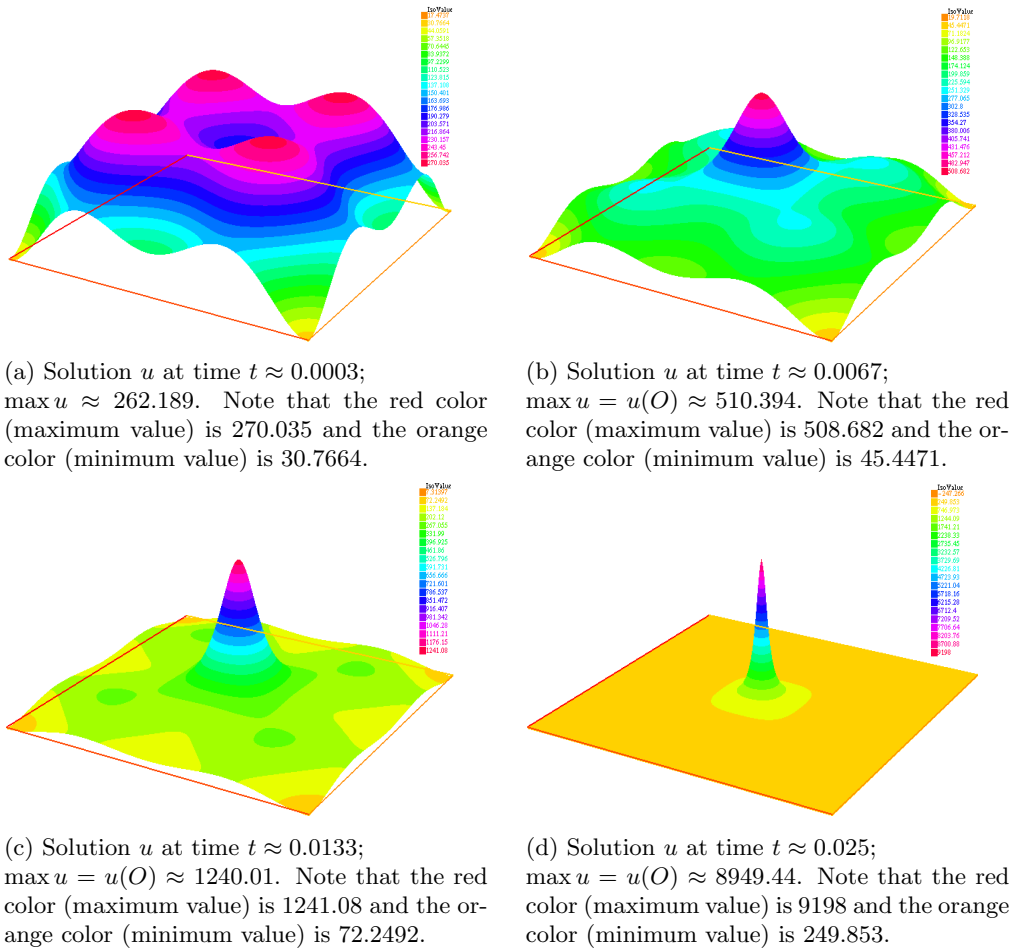


Figure 3.22: Test *IFT – Test₂*: numerical solution. Evolution of u and its graphical representation: with t increasing the value of u at O increases and the values of u in P_1, P_2, P_3 and P_4 decrease, even with the same behaviors.

of the term $k_1 = -0.2$. Let us fix then

$$\begin{cases} k_0 = 1, k_2 = k_4 = 1, k_3 = 0.1, \\ u_0(\mathbf{x}) = 1.15^{-(x^2+y^2)}(4-x^2)(4-y^2)^2, \quad v_0(\mathbf{x}) = 0.55e^{-(x^2+y^2)}(4-x^2)^2(4-y^2)^2. \end{cases}$$

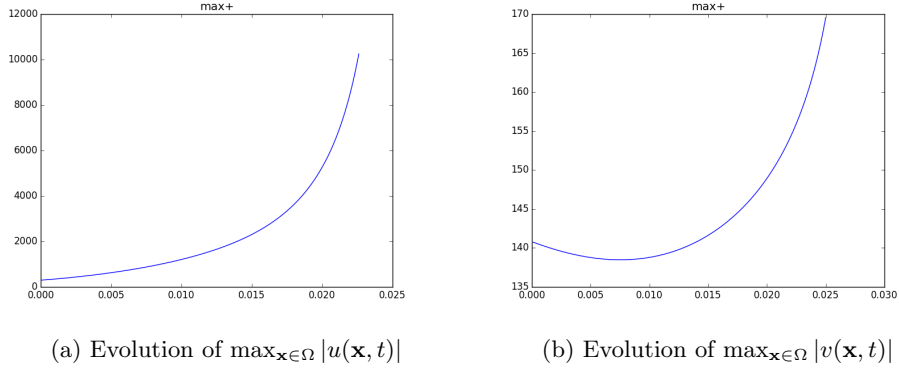


Figure 3.23: Test $DDT - Test_1$: Analysis of the behaviors of $u(\mathbf{x}, t)$ and $v(\mathbf{x}, t)$

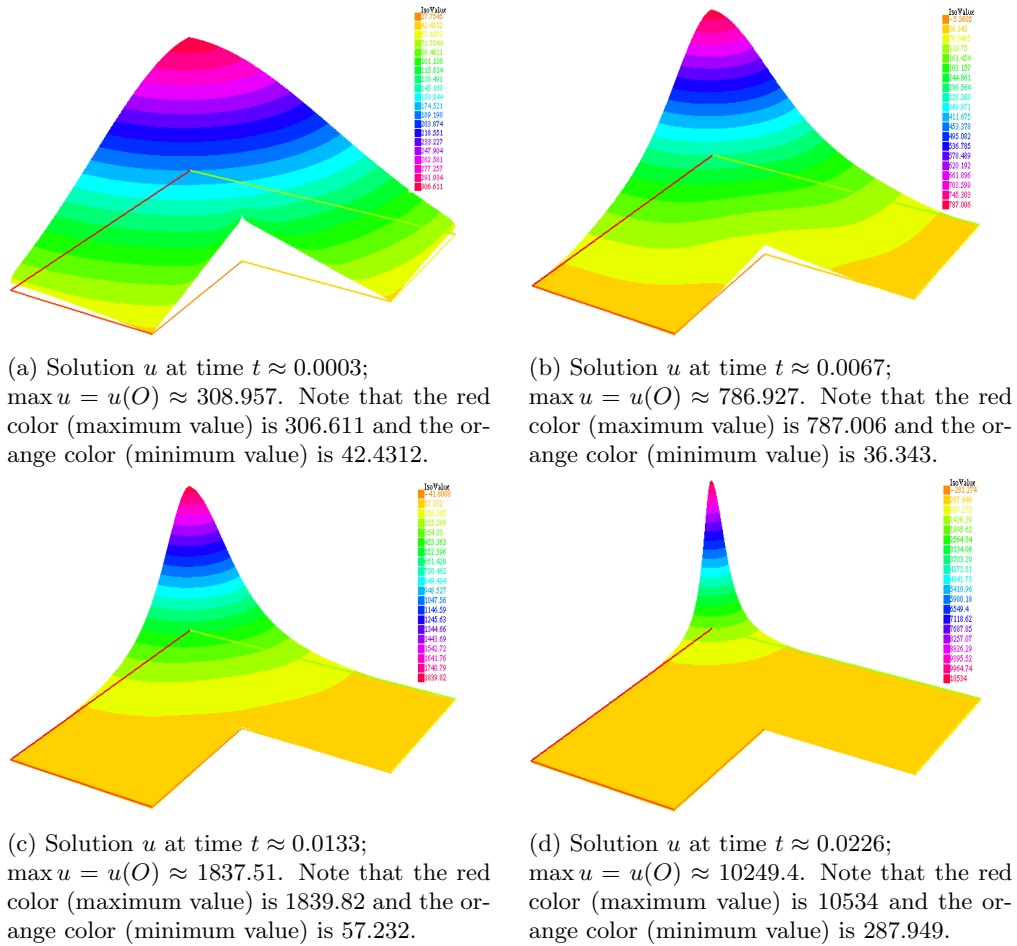


Figure 3.24: Test $DDT - Test_1$: numerical solution. Evolution of u and its graphical representation: with t increasing the value of u at O increases. According to the blow-up criterion given at page 21, u blows-up at $t \approx 0.0226$.

Remark 9. Observing Figure 3.28, we can see that unlike the other cases, the maximum of the initial

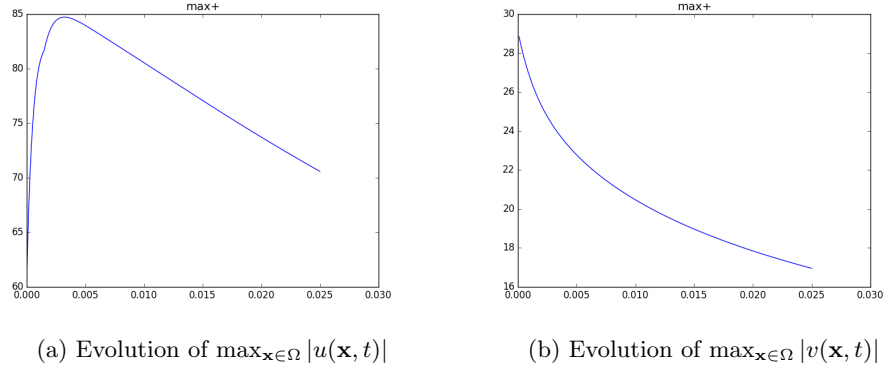


Figure 3.25: Test $DDT - Test_2$: Analysis of the behaviors of $u(\mathbf{x}, t)$ and $v(\mathbf{x}, t)$

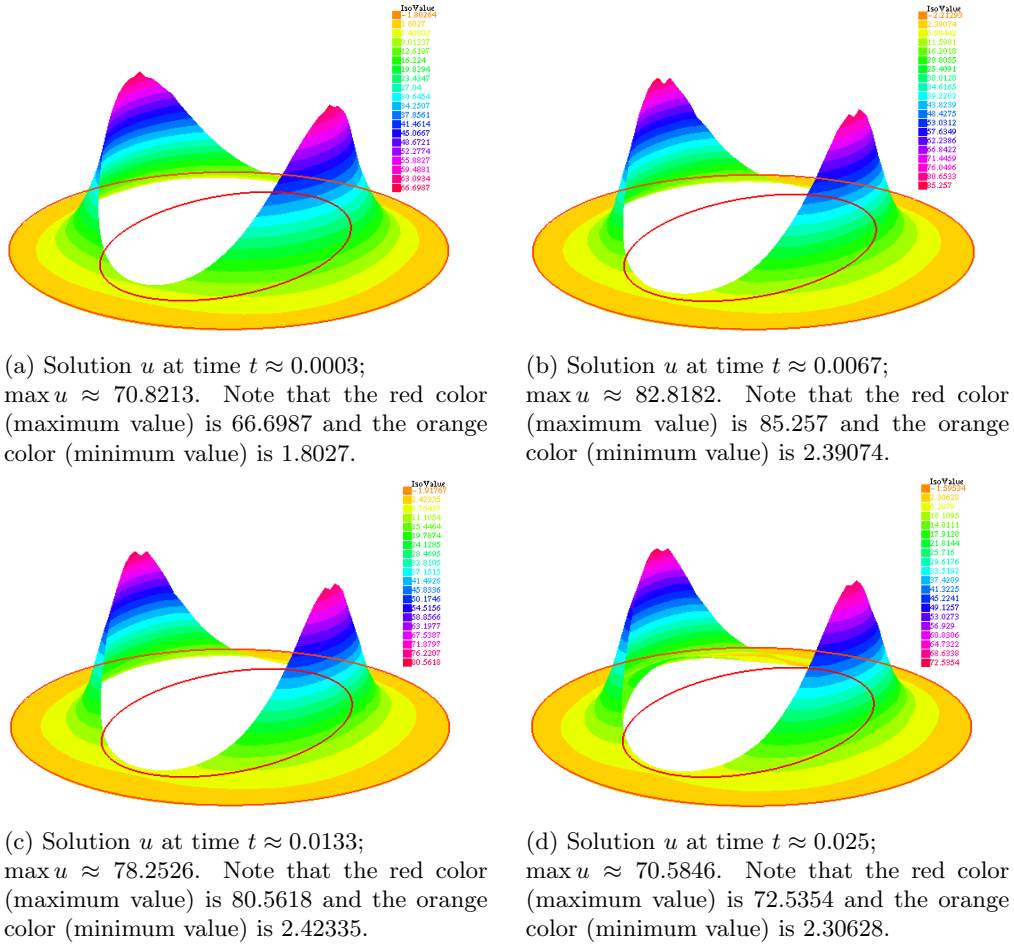


Figure 3.26: Test $DDT - Test_1$: numerical solution. Evolution of u and its graphical representation.

data u_0 , centered in this test in the origin of the domain, is not maintained in the succeeding iterations.

Indeed, it is shown in the intermediate phases that such a maximum of u_0 decreases in the origin, achieving a minimum (see Sub-Figure 3.29b), and then increases again (see Sub-Figure 3.28d). On the other hand the maximum of the solution is distributed on a circular crown.

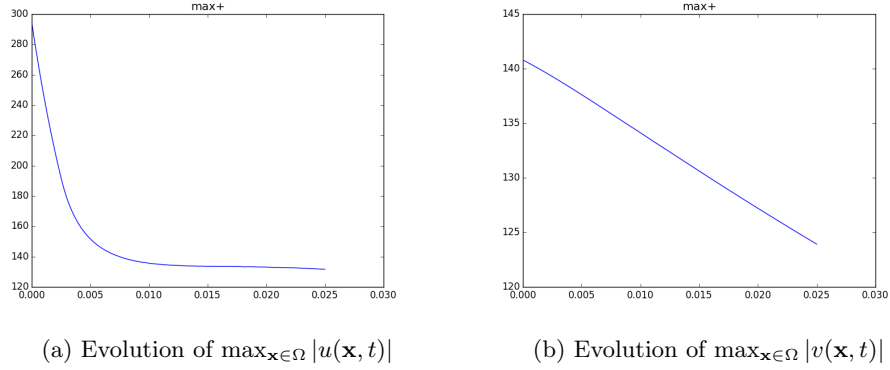


Figure 3.27: Analysis of the behaviors of $u(\mathbf{x}, t)$ and $v(\mathbf{x}, t)$

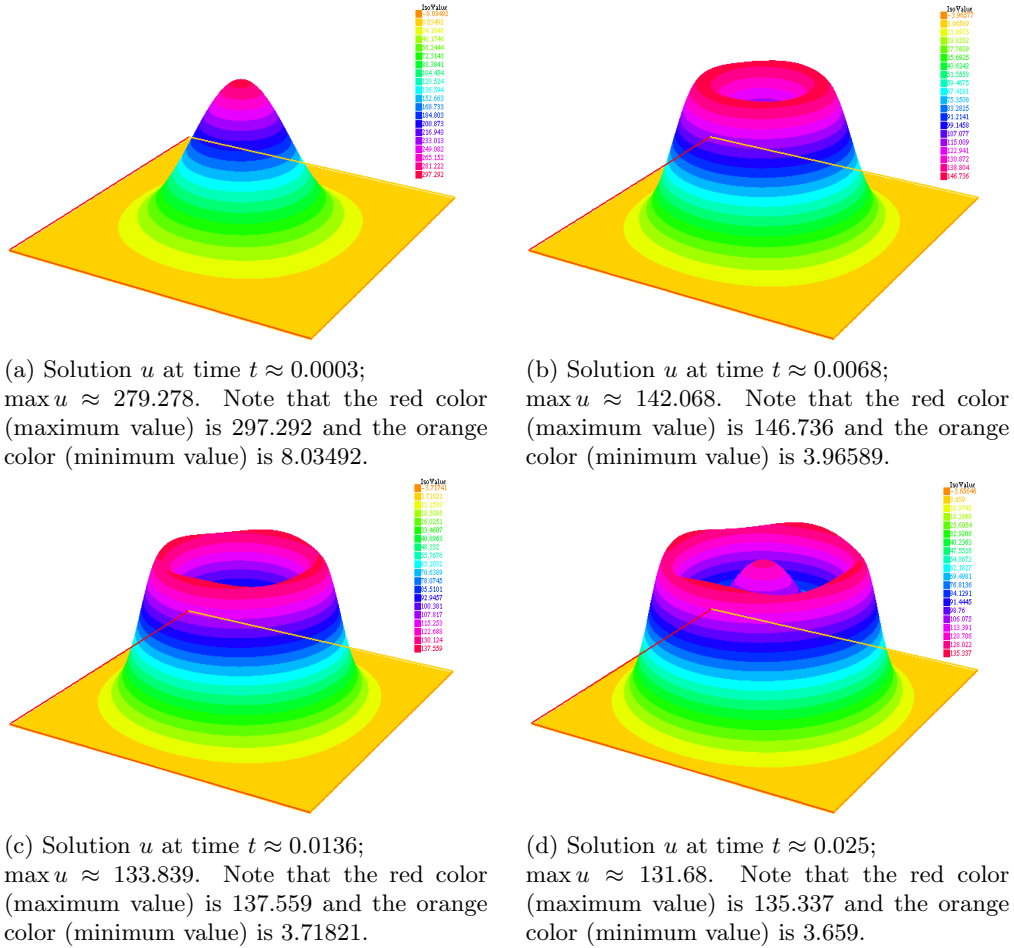


Figure 3.28: Test *NegSensi – Test₁*: numerical solution. Evolution of u and its graphical representation.

Remark 10. For completeness of information, we include also the pictures of the meshes used in our simulations, where the number of vertices and triangles are specified; this information is shown in Figures 3.30a, 3.30b and 3.30c. We outline that the performed tests are not very responsive to mesh thickening, in the sense that a refining of a mesh infers a solution qualitatively coherent with that obtained with a poorer mesh. In this sense, since on the contrary the computational time considerably increases with the

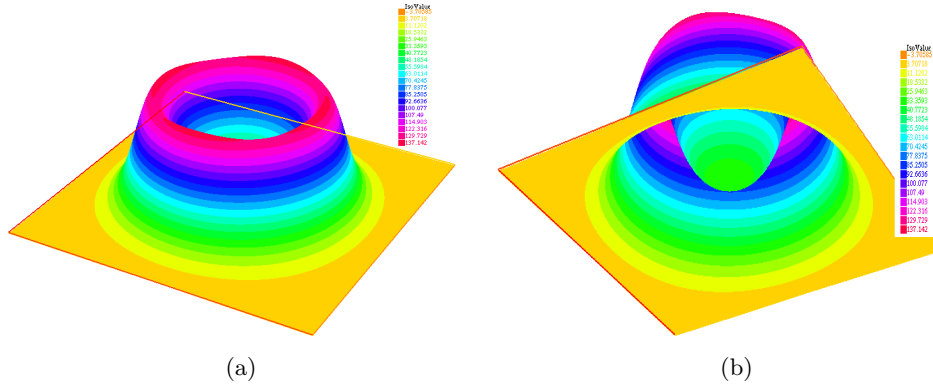


Figure 3.29: Test *NegSensi* – $Test_1$: view of two different iterations of the intermediate phase from as many different perspectives.

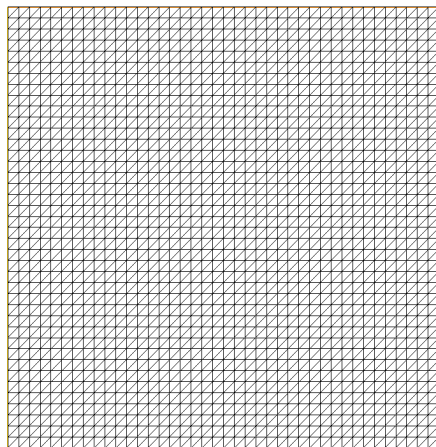
number of triangles and vertices, we believe that the used discretization is sufficient for our purposes.

For a more complete picture, we conclude our analysis by reporting below four tables; they include some tests for which, unless specified, the same general assumptions made in the introduction to the §3.2.1 are considered. To be precise, and specially in terms of the conservation mass property explained in Proposition 2.6, some of these tests aim at emphasizing the influence of the mass m and/or the the cross-diffusion term k_1 on the behavior of the solution, in particular the cell distribution. It is worth to say that, in order to interpret the corresponding results, we have to take in mind the blow-up criterion described at page 21.

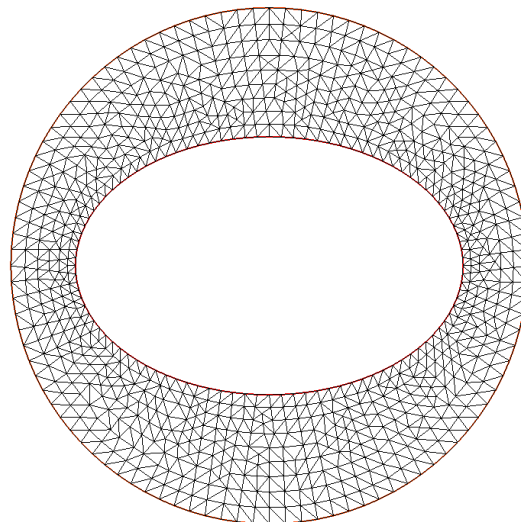
- Table 3.1: In the first table we fix the values of k_i for $i = 0, 2, 3, 4$. In particular $k_0 = 1$, $k_2 = 1$, $k_3 = 0.1$, $k_4 = 1$ and let us vary the coefficient k_1 .
As we can see when k_1 increases and $k_i = 0, 2, 3, 4$ remain fixed, the blow-up time decreases.
- Table 3.2: In the second table we fix the values of k_i for $i = 1, 2, 3, 4$. In particular $k_1 = 0.2$, $k_2 = 1$, $k_3 = 0.1$, $k_4 = 1$ and let us vary the coefficient k_0 .
Note that if k_0 increases the blow-up time increases. Since k_0 the diffusion coefficient of Δu , the model in this sense is consistent.
- Table 3.3: In the third table we fix the values of k_i for $i = 0, 1, 2, 3$. In particular $k_0 = 1$, $k_1 = 0.2$, $k_2 = 1$, $k_3 = 0.1$ and let us vary the coefficient k_4 .
The chemoattractant it is also produced by the bacteria with rate k_4 , so it is normal that if this coefficient increases, the blow-up time decreases.
- Table 3.4.: In the fourth table we fix the values of k_i for $i = 0, 1, 2, 4$. In particular $k_0 = 1$, $k_1 = 0.2$, $k_2 = 1$, $k_4 = 1$ and let us vary the coefficient k_3 .
In the system (3.4) the chemoattractant decays with rate k_3 , therefore the fact that if k_3 increases, the time of the blow-up slowly increases is consistent with the model.

In the Table 3.5, we propose a summary table of tests performed leaving the k_i for $i = 0, 1, 2, 3, 4$ fixed and modifying the initial function $u_0(\mathbf{x})$.

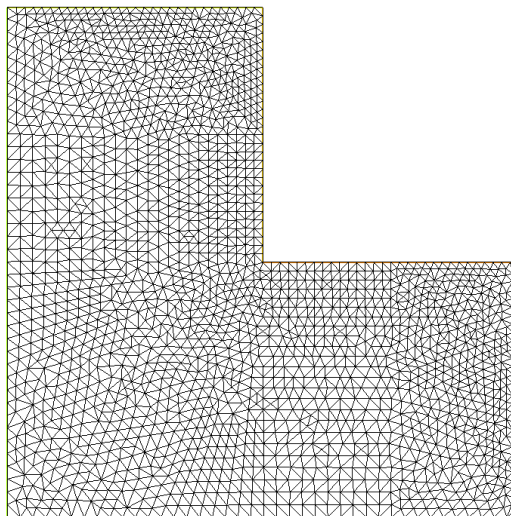
Note that if $\int_{\Omega} u_0(\mathbf{x})$ increases the blow-up time decreases.



(a) Square mesh : triangles 320, vertices 1681



(b) Crown mesh: triangles 1624, vertices 912



(c) Starred mesh: triangles 4092, vertices 2147

k_1	t^*	Properties of the u -component
0.01	0.025	global solution: $t^* = \infty$
0.1	0.025	global solution: $t^* = \infty$
0.4	0.0103	blowing up local solution: $t^* = 0.0103$
0.5	0.0095	blowing up local solution: $t^* = 0.0095$

Table 3.1: Influence of the cross-diffusion term k_1 on the behaviour of the u -component: global solution or blowing up solution at t^*

k_0	t^*	Properties of the u -component
0.3	0.0224	blowing up local solution: $t^* = 0.0224$
1	0.0226	blowing up local solution: $t^* = 0.0226$
1.5	0.025	global solution
2	0.025	global solution

Table 3.2: Influence of the term k_0 on the behaviour of the u -component: global solution or blowing up solution at t^*

k_4	t^*	Properties of the u -component
0.3	0.025	global solution
0.5	0.025	global solution
1	0.0226	blowing up local solution: $t^* = 0.0226$
2	0.0176	blowing up local solution: $t^* = 0.0176$

Table 3.3: Influence of the term k_4 on the behaviour of the u -component: global solution or blowing up solution at t^*

k_3	t^*	Properties of the u -component
2	0.023	blowing up local solution: $t^* = 0.023$
5	0.0236	blowing up local solution: $t^* = 0.0236$
15	0.025	global solution
20	0.025	global solution

Table 3.4: Influence of the term k_4 on the behaviour of the u -component: global solution or blowing up solution at t^*

$u_0(\mathbf{x})$	$\int_{\Omega} u_0(\mathbf{x})$	Properties of the u -component
$0.8e^{(-x^2-y^2)}(4-x^2)^2(4-y^2)^2$	408.053	global solution
$0.9e^{(-x^2-y^2)}(4-x^2)^2(4-y^2)^2$	459.06	global solution
$e^{(-x^2-y^2)}(4-x^2)^2(4-y^2)^2$	510.067	blowing up local solution: $t^* = 0.0243$
$1.15e^{(-x^2-y^2)}(4-x^2)^2(4-y^2)^2$	586.577	blowing up local solution: $t^* = 0.0226$
$1.75e^{(-x^2-y^2)}(4-x^2)^2(4-y^2)^2$	892.617	blowing up local solution: $t^* = 0.0183$
$2e^{(-x^2-y^2)}(4-x^2)^2(4-y^2)^2$	1020.13	blowing up local solution: $t^* = 0.0172$

Table 3.5: Influence of the size of the mass m on the behaviour of the u -component: global solution or blowing up solution at t^*

Chapter 4

General conclusions and future works

In this thesis we have studied a model coming from bio-mathematics and described by a system of two coupled differential equations. The formulation idealizes the so called *chemotaxis*, a phenomenon according to which some species directs its movement by virtue of the presence of a chemical signal in the same environment. By the mathematical point of view, it is precisely the interplay between the distributions of the population and the chemical that makes the problem complex and challenging. Indeed, during the last decades, many researchers have been analyzing this field and throughout the time many questions are positively addressed whilst other remain open.

The original chemotaxis model is attributed to the scientists Keller and Segel, who proposed two pioneer formulations of the mathematical model. The main difference between these formulations is essentially tied to the influence of the population on the chemical; specifically, in a *chemo-production model* the cells produce the signal whilst in the *chemo-consumption model* the cells consume the signal. Such situations are translated in so many mathematical formulations, where the so-called cross-diffusive term (chemo-sensitivity) measures the power of the interaction between the population and the chemical and essentially destabilizes the effect of the diffusion for the evolution of the cells distribution. To be more precise, real experiments show that the general behavior of the cells throughout the time is, in general, far to be regular and homogeneous: indeed, if from one hand the diffusion tends to stabilize the evolution of the cells, the counterpart given by the interaction population-chemical breaks this equilibrium tendency. So, from that, different scenarios are possible: homogeneous or heterogeneous distribution for the cells in time, pattern formations and/or aggregation phenomena in one or more points of the environment (chemotactic collapse).

As far as this report is concerned, we herein limited our interest in considering the classical Keller–Segel model, that is a production model presenting a chemo-sensitivity which is a linear function of the cells distribution. Moreover, such chemo-sensitivity is oppositely directed to the direction of the diffusion. This idealizes the situation where the cells are attracted by the chemical, so that an increase of the chemical somehow produces a similar increase for the cells. Additionally, we confined our study to two- and three-dimensional domains, which in particular are totally insulated; this leads to a coupled-system of parabolic equations with Neumann boundary conditions.

In order to provide a more general and comprehensive picture of the general problem we dedicated to both theoretical and numerical analysis of the problem, giving a certain importance to unbounded solutions. More exactly, as to the theoretical approach we considered two main results which infer lower bounds for the blow-up time of such solutions; on the other hand, we largely illustrated some numerical examples, simulated by a mixed Finite-Element (in space) and Finite-Difference (in time) method. These simulations, which have been of great support, show properties of the solutions which are not straightforwardly achievable by a simple theoretical analysis. In this direction, it is worst to mention that the easiest repulsion model deals with the same problem described above when the directions of

CHAPTER 4. GENERAL CONCLUSIONS AND FUTURE WORKS

the diffusion and the chemo-sensitivity coincide. In this case, the cells are repelled so that the blow-up phenomena is not naturally expected. The theoretical analysis is so far rather poor, in view of its complexity; in particular we did not spend any comments on it. Conversely, we discussed some numerical cases concerning with complex this situation.

Even though in this thesis we did not confine to summarize and list the main results concerning this interesting field, but conversely we also dedicated time to a number of numerical experiments, we are aware about the great difficulties (both theoretical and numerical) linked to the general comprehension of the problem. In this sense, further and natural works arising from this report are connected to cases where other expressions of the diffusion and/or the sensitivity define the problem. We can imagine, for instance nonlinear diffusion expression for the cells distribution, singular cross-diffusive terms, presence of logistic-sources for the evolution equations of the species, different boundary conditions and so on.

Bibliography

- [1] G. Acosta, R. G. Duran and J. D. Rossi. An adaptive time step procedure for a parabolic problem with blow-up. *Computing*, **68**: 343-373, 2002.
- [2] G. Allaire. *Numerical Analysis and Optimization. An Introduction to Mathematical Modelling and Numerical Simulation*. Oxford science publications, 2007.
- [3] C. Bandle and H. Brunner. Blow-up in diffusion equations: A survey. *J. Comput. Appl. Math.*, **97**: 3-22, 1998.
- [4] N. Bellomo, A. Bellouquid, J. Nieto and J. Soler. Multiscale biological tissue models and flux-limited chemotaxis for multicellular growing systems. *Math. Models Methods Appl. Sci.*, **20**(7): 1179-1207, 2010.
- [5] N. Bellomo, A. Bellouquid, Y. Tao and M. Winkler. Toward a mathematical theory of Keller-Segel models of pattern formation in biological tissues. *Mathematical Models and Methods in Applied Sciences*, **25**(9): 1663-1763, 2015.
- [6] N. Bellomo and M. Winkler. A degenerate chemotaxis system with flux limitation: Maximally extended solutions and absence of gradient blow-up. *Comm. Part. Diff. Eq.*, **42**(3): 436-473, 2017.
- [7] P. Biler. Local and global solvability of some parabolic systems modelling chemotaxis. *Adv. Math.Sci. Appl.*, **8**(2): 715-743, 1998.
- [8] Haim, Brezis. *Analisi funzionale, teoria e applicazioni, con un'appendice su integrazione astratta di Carlo Sbordone*. Liguori Editore, 1986.
- [9] M. C. Carrisi. A further condition in the extended macroscopic approach to relativistic gases. *Int. J. Pure Appl. Math.*, **67**: 259-289, 2011.
- [10] M. C. Carrisi and S. Mignemi. Snyder-de Sitter model from two-time physics. *Phys. Rev. D.*, **82**: 5 pages, 2010.
- [11] T. Cieřlak and C. Stinner. Finite-time blowup and global-in-time unbounded solutions. *J. Differential Equations*, **252**(10): 5832-5851, 2012.
- [12] T. Cieřlak and C. Stinner. New critical exponents in a fully parabolic quasilinear Keller-Segel system and applications to volume filling models. *J. Differential Equations*, **258**(6): 2080-2113, 2015.
- [13] FreeFem: A high level multiphysics finite element software. *Link:*<http://www.freefem.org/ff++>.
- [14] FreeFem: A high level multiphysics finite element software. *Wikipedia:* <https://en.wikipedia.org/wiki/FreeFem>.
- [15] K. Fujie, M. Winkler, and T. Yokota. Boundedness of solutions to parabolic-elliptic Keller-Segel systems with signal-dependent sensitivity. *Math. Methods Appl. Sci.*, **38**(6): 1212-1224, 2015.

BIBLIOGRAPHY

- [16] T. Hillen and K. J. Painter. A user's guide to PDE models for chemotaxis. *J. Math. Biol.*, **58**: 183-217, 2009.
- [17] History of chemotaxis research. *Wikipedia*: <http://en.wikipedia.org/wiki/Chemotaxis>.
- [18] D. Horstmann. From 1970 until present: the Keller-Segel model in chemotaxis and its consequences, part 1. *Jahresber. Deutsch. Math.-Verein*, **105**(3): 103-165, 2003.
- [19] D. Horstmann and Winkler. Boundedness vs. blow-up in a chemotaxis system. *J. Differential Equations*, **215**(1): 52-107, 2005.
- [20] W. Jäger and S. Luckhaus. On explosions of solutions to a system of partial differential equations modelling chemotaxis. *T. Am. Math. Soc.*, **329**(2): 819-824, 1992.
- [21] E. F. Keller and L. A. Segel. Initiation of slime mold aggregation viewed as an instability. *J. Theoret. Biol.*, **26**: 399-415, 1970.
- [22] E. F. Keller and L. A. Segel. Traveling bands of chemotactic bacteria: A theoretical analysis. *J. Theoret. Biol.*, **30**(2): 235, 1971.
- [23] J. Lankeit. Eventual smoothness and asymptotics in a three- dimensional chemotaxis system with logistic source. *J. Differential Equations*, **258**(4): 1158-1191, 2015.
- [24] J. Lankeit. Locally bounded global solutions to a chemotaxis consumption model with singular sensitivity and nonlinear diffusion. *J. Differential Equations*, **262**(7): 4052-4084, 2017.
- [25] S. Larsson and V. Thome. Partial differential Equations with Numerical Methods. *Springer-Verlag*, 2003.
- [26] D. Liu. Global classical solution to a chemotaxis consumption model with singular sensitivity. *Nonlinear. Anal. Real World Appl.*, **41**: 497-508, 2018.
- [27] M. Marras. Bounds for blow-up time in nonlinear parabolic systems under various boundary conditions. *Num. Funct. Anal. Optim.*, **32**: 453-468, 2011.
- [28] M. Marras, S. Vernier Piro and G. Viglialoro. Estimate from below of blow-up time in a parabolic system with gradient term. *Int. J. Pure Appl. Math.*, **93**: 297-306, 2014.
- [29] M. Marras, S. Vernier Piro and G. Viglialoro. Lower bounds for blow-up in a parabolic-parabolic Keller-Segel system. *Submitted*.
- [30] M. Marras and S. Vernier Piro. Blow-up phenomena in reaction-diffusion systems. *Discret. Contin. Dyn. Syst.*, **32**: 4001-4014, 2012.
- [31] M. Marras and S. Vernier Piro. Bounds for blow-up time in nonlinear parabolic systems. *Discret. Contin. Dyn. Syst. Suppl.*, 1025-1031, 2011.
- [32] T. Nagai. Blowup of nonradical solutions to parabolic-elliptic systems modeling chemotaxis in two-dimensional domains. *J. Inequal. Appl.*, **6**(1): 37-55, 2001.
- [33] T. Nagai and T. Senba. Global existence and blow-up of radial solutions to a parabolic-elliptic system of chemotaxis. *Adv. Math. Sci. Appl.*, **8**(1): 145-156-55, 1998.
- [34] C. D. Pagani, S.Salsa. *Analisi Matematica*. Zanichelli. Volume 2. 2012.
- [35] L. E. Payne and G. A. Philippin. Blow-up phenomena for a class of parabolic systems with time dependent coefficients. *Appl. Math.* **3**: 325-330, 2012.

BIBLIOGRAPHY

- [36] L. E. Payne and G. A. Philippin and S. Vernier-Piro. Blow-up phenomena for a semilinear heat equation with nonlinear boundary condition, II. *Nonlinear Analysis-Theor.*, **73**: 971-978, 2010.
- [37] L. E. Payne and J.C. Song. Lower bounds for blow-up in a model of chemotaxis. *J. Math. Anal. Appl.*, **385**: 672-676, 2012.
- [38] L. E. Payne and P. W. Schaefer. Lower bound for blow-up time in parabolic problems under Neumann conditions. *Appl. Anal.*, **85**: 1301-1311, 2006.
- [39] B. Roberts, E. Chung, Sheng-Han Yu and Shang-Zhong Li. Keller-Segel Models for Chemotaxis. *Mathematical Method of Bioengineering Group Presentation*.
- [40] B. D. Sleeman and H. A. Levine. Partial differential equations of chemotaxis and angiogenesis. *Math. Methods Appl. Sci.*, **24**(6): 405-426, 2001.
- [41] A. Stevens and H. G. Othmer. Aggregation, blowup and collapse: The abc's of taxis in reinforced random walks. *SIAM J. Appl. Math.*, **57**(4): 1044-1081, 1997.
- [42] Y. Tao L. Wang, and Z.-A. Wang. Large time behavior of a parabolic-parabolic chemotaxis model with logarithmic sensitivity in one dimension. *Discrete Continuous Dyn. Syst. Ser. B.*, **18**(3): 821-845, 2013.
- [43] Y. Tao and M. Winkler. Boundedness in a quasilinear parabolic-parabolic Keller-Segel system with subcritical sensitivity. *J. Differential Equations*, **252**(1): 692-715, 2012.
- [44] G. Viglialoro. Boundedness properties of very weak solutions to a fully parabolic chemotaxis-system with logistic source. *Nonlinear Anal. Real World Appl.*, **34**: 520-535, 2017.
- [45] G. Viglialoro. On the blow-up time of a parabolic system with damping terms. *C. R. Acad. Bulg. Sci.*, **67**: 1223-1232, 2014.
- [46] G. Viglialoro and T. Woolley. Eventual smoothness and asymptotic behaviour of solutions to a chemotaxis system perturbed by a logistic growth. *Discrete Continuous Dyn. Syst. Ser. B.*, **22**(5), 2017.
- [47] M. Winkler. Finite-time blow-up in low-dimensional Keller-Segel systems with logistic-type super-linear degradation. *Z. Angew. Math. Phys.*, **69**(40): 2018.

Appendix A

Some essential results on theoretical analysis

Let us briefly give some well-known results within the general Mathematical Analysis theory.

A.1 Overview on the L^p spaces

Let $(\Omega, \mathcal{M}, \mu)$ denote a measure space, i.e., Ω is a set and

(i) \mathcal{M} is a σ -algebra in Ω , i.e., \mathcal{M} is a collection of Ω such that:

(a) $\emptyset \in \mathcal{M}$,

(b) $A \in \mathcal{M} \Rightarrow A^c \in \mathcal{M}$,

(c) $\cup_{n=1}^{\infty} A_n \in \mathcal{M}$ whenever $A_n \in \mathcal{M} \forall n$,

(ii) μ is a measure, i.e., $\mu : \mathcal{M} \rightarrow [0, \infty]$ satisfies

(a) $\mu(\emptyset) = 0$,

(b) $\mu(\cup_{n=1}^{\infty} A_n) = \sum_{n=1}^{\infty} \mu(A_n)$ whenever A_n is a disjoint countable family of members of \mathcal{M} .

The members of \mathcal{M} are called the measurable sets.

(iii) Ω is σ -finite, i.e., there exists a countable family (Ω_n) in \mathcal{M} such that $\Omega = \cup_{n=1}^{\infty} \Omega_n$ and $\mu(\Omega_n) < \infty \forall n$.

The sets $E \in \mathcal{M}$ with the property that $\mu(E) = 0$ are called the null sets. We say that a property holds a.e. (or for almost all $x \in \Omega$) if it holds everywhere on Ω except on a null set.

We denote by $L^1(\Omega, \mu)$, or simply $L^1(\Omega)$, the space of integrable functions from Ω into \mathbb{R} .

A.1.1 Definition and elementary properties of L^p spaces: main inequalities

Definition A.1. Let $p \in \mathbb{R}$ with $1 < p < \infty$; we set

$$L^p(\Omega) = \{f : \Omega \rightarrow \mathbb{R}; f \text{ is measurable and } |f|^p \in L^1(\Omega)\}$$

with

$$\|f\|_L^p = \|f\|_p = \left[\int_{\Omega} |f(x)|^p d\mu \right]^{1/p}.$$

Definition A.2. We set

APPENDIX A. SOME ESSENTIAL RESULTS ON THEORETICAL ANALYSIS

$$L^\infty(\Omega) = \left\{ f : \Omega \rightarrow \mathbb{R}, f \text{ is measurable and there is a constant } C \text{ such that } |f(x)| \leq C \text{ a.e. on } \Omega \right\}$$

with

$$\|f\|_L^\infty = \|f\|_\infty = \inf\{C; |f(x)| \leq C \text{ a.e. on } \Omega\}.$$

Notation. Let $1 \leq p \leq \infty$; we denote by p' the conjugate exponent,

$$\frac{1}{p} + \frac{1}{p'} = 1.$$

Theorem A.1 (Hölder's inequality.). *Assume that $f \in L^p$ and $g \in L^{p'}$ with $1 \leq p \leq \infty$. Then $fg \in L^1$ and*

$$\int |fg| \leq \|f\|_p \|g\|_{p'}. \quad (\text{A.1})$$

In the case $p = p' = 2$ we recover the well-known Cauchy–Shwarz inequality.

A.2 Sobolev spaces: definitions and elementary properties of $W^{1,p}(\Omega)$

Let $\Omega \subset \mathbb{R}^N$ be an open set and let $p \in \mathbb{R}$ with $1 \leq p \leq \infty$.

Definition A.3. *The Sobolev space $W^{1,p}(\Omega)$ is defined by*

$$W^{1,p}(\Omega) = \left\{ u \in L^p(\Omega) \mid \exists g_1, g_2, \dots, g_N \in L^p(\Omega) \text{ such that } \int_\Omega u \frac{\partial \phi}{\partial x_i} = - \int_\Omega g_i \phi \quad \forall \phi \in C_c^\infty(\Omega), \quad \forall i = 1, 2, \dots, N \right\}$$

We set

$$H^1(\Omega) = W^{1,2}(\Omega)$$

For $u \in W^{1,p}(\Omega)$ we define $\frac{\partial u}{\partial x_i} = g_i$, and we write

$$\nabla u = \text{grad } u = \left(\frac{\partial u}{\partial x_1}, \frac{\partial u}{\partial x_2}, \dots, \frac{\partial u}{\partial x_N} \right).$$

The space $W^{1,p}(\Omega)$ is equipped with the norm

$$\|u\|_{W^{1,p}} = \|u\|_{L^p} + \sum_{i=1}^N \left\| \frac{\partial u}{\partial x_i} \right\|_{L^p},$$

or sometimes with the equivalent norm

$$\left(\|u\|_{L^p}^p + \sum_{i=1}^N \left\| \frac{\partial u}{\partial x_i} \right\|_{L^p}^p \right)^{\frac{1}{p}}.$$

The space $H^1(\Omega)$ is equipped with the scalar product

$$(u, v)_{H^1} = (u, v)_{L^2} + \sum_{i=1}^N \left(\frac{\partial u}{\partial x_i}, \frac{\partial v}{\partial x_i} \right)_{L^2},$$

the associated norm

$$\|u\|_{H^1} = \left(\|u\|_{L^2}^2 + \sum_{i=1}^N \left\| \frac{\partial u}{\partial x_i} \right\|_{L^2}^2 \right)^{\frac{1}{2}},$$

is equivalent to the $W^{1,2}$ norm.

A.2.1 The space $W_0^{1,p}$

Definition A.4. Let $1 < p < \infty$; $W_0^{1,p}$ denotes the closure of $C_c^1(\Omega)$ in $W^{1,p}$. Set

$$H_0^1(\Omega) = W_0^{1,2}(\Omega).$$

The functions in $W_0^{1,p}(\Omega)$ are “roughly” those of $W^{1,p}(\Omega)$ that “vanish on $\partial\Omega$ ”.

We denote by $W^{-1,p'}(\Omega)$ the dual space of $W_0^{1,p}(\Omega)$, $1 \leq p < \infty$, and by $H^{-1}(\Omega)$ the dual of $H_0^1(\Omega)$. The dual of $L^2(\Omega)$ is identified with $L^2(\Omega)$, but we do not identify $H_0^1(\Omega)$ with its dual. We have the inclusions

$$H_0^1(\Omega) \subset L^2(\Omega) \subset H^{-1}(\Omega),$$

where these injections are continuous and dence.

If Ω is bounded then

$$W_0^{1,p}(\Omega) \subset L^2(\Omega) \subset W^{-1,p'}(\Omega),$$

if $\frac{2N}{N+2} \leq p < \infty$, with continuous and dence injections. If Ω is not bounded, the same holds, but only for the range $\frac{2N}{N+2} \leq p \leq 2$.

The element of $W^{-1,p'}$ are completely described by the following result:

Lemma A.2. Let $F \in W^{-1,p'}(\Omega)$. Then there exist functions $f_0, f_1, f_2, \dots, f_N \in L^{p'}(\Omega)$ such that

$$\langle F, v \rangle = \int_{\Omega} f_0 v + \sum_{i=1}^N \int_{\Omega} f_i \frac{\partial v}{\partial x_i} \quad \forall v \in W_0^{1,p}(\Omega),$$

$$\|F\| = \max_{0 \leq i \leq N} \|f_i\|_{p'}.$$

If Ω is bounded we can take $f_0 = 0$.

A.2.2 Some Sobolev type inequalities

Lemma A.3. Sobolev type inequality Let v be a non negative C^1 function, defined in a bounded domain $\Omega \in \mathbb{R}^3$ with the origin inside, assumed to be star-shaped and convex in two orthogonal directions. Then

$$\int_{\Omega} v^{\frac{3n}{2}} d\mathbf{x} \leq \left[\frac{3}{2p_0} \int_{\Omega} v^n d\mathbf{x} + \frac{n}{2} \left(1 + \frac{d}{p_0} \right) \int_{\Omega} v^{n-1} |\nabla v| d\mathbf{x} \right]^{\frac{3}{2}} \quad (\text{A.2})$$

valid for $n \geq 1$, with $p_0 := \min_{\partial\Omega} (\mathbf{x} \cdot \nu)$ and $d := \max_{\bar{\Omega}} |\mathbf{x}|$

From (A.2) we derive a bounded for $\int_{\Omega} v^3 d\mathbf{x}$, to be used in the proof on the main theorem.

Lemma A.4. Under the hypotheses of (A.2)

$$\int_{\Omega} v^3 d\mathbf{x} \leq \sqrt{2} \left[m_1^{\frac{3}{2}} \left(\int_{\Omega} v^2 d\mathbf{x} \right)^{\frac{3}{2}} + \frac{m_2^{\frac{3}{2}}}{4\varepsilon^3} \left(\int_{\Omega} v^2 d\mathbf{x} \right)^3 + \frac{3}{4} m_2^{\frac{3}{2}} \varepsilon \int_{\Omega} |\nabla v|^2 d\mathbf{x} \right] \quad (\text{A.3})$$

with $m_1 := \frac{3}{2p_0}$, $m_2 := 1 + \frac{d}{p_0}$ and ε an arbitrary positive function.

Proof. We point out that (A.3) can be derived by (A.2). We use (A.2) with $n = 2$ and by using Schwarz inequality in the second integral, we get

$$\int_{\Omega} v^3 d\mathbf{x} \leq \left[m_1 \int_{\Omega} v^2 d\mathbf{x} + m_2 \left(\int_{\Omega} v^2 d\mathbf{x} \right)^{\frac{1}{2}} \left(\int_{\Omega} |\nabla v|^2 \right)^{\frac{1}{2}} d\mathbf{x} \right]^{\frac{3}{2}}$$

APPENDIX A. SOME ESSENTIAL RESULTS ON THEORETICAL ANALYSIS

By applying first the arithmetic inequality $(a + b)^{\frac{3}{2}} \leq \sqrt{2}(a^{\frac{3}{2}} + b^{\frac{3}{2}})$, valid with $a, b > 0$, and the Hölder inequality, we obtain

$$\begin{aligned} \int_{\Omega} v^3 d\mathbf{x} &\leq \sqrt{2} \left[m_1^{\frac{3}{2}} \left(\int_{\Omega} v^2 d\mathbf{x} \right)^{\frac{3}{2}} + m_2^{\frac{3}{2}} \left[\left(\int_{\Omega} v^2 d\mathbf{x} \right)^3 \right]^{\frac{1}{4}} \left(\int_{\Omega} |\nabla v|^2 \right)^{\frac{3}{4}} d\mathbf{x} \right] \\ &\leq \sqrt{2} \left[m_1^{\frac{3}{2}} \left(\int_{\Omega} v^2 d\mathbf{x} \right)^{\frac{3}{2}} + m_2^{\frac{3}{2}} \left[\frac{1}{4\varepsilon^3} \left(\int_{\Omega} v^2 d\mathbf{x} \right)^3 + \frac{3}{4} \varepsilon \int_{\Omega} |\nabla v|^2 d\mathbf{x} \right] \right] \end{aligned}$$

where in the last inequality we use

$$a^r b^{1-r} \leq ra + (1-r)b, a, b > 0, 0 < r < 1, \tag{A.4}$$

and ε is any positive function; the lemma is so proved. \square

Appendix B

Some essential results on numerical analysis

B.1 Numerical methods for parabolic equations

Let us focus on some fundamental theoretical results for the numerical resolution of parabolic problems.

As a classical model of parabolic equations, we consider the following heat equation and study corresponding finite difference methods and finite element methods

$$\begin{cases} u_t - \Delta u = f & \text{in } \Omega \times (0, T), \\ u = 0 & \text{on } \partial\Omega \times (0, T), \\ u(x, 0) = u_0 & \text{in } \Omega. \end{cases} \quad (\text{B.1})$$

Here $u = u(x, t)$ is a function of spatial variable $x \in \Omega$ and time variable $t \in (0, T)$ and the Laplace differential operator Δ is taking with respect to the spatial variable.

B.2 Variational formulation

The first attempt is to multiply by a test function $v \in H_0^1(\Omega)$ the first equation of (B.1) and apply the integration by part. We obtain a this variational formulation: given an $f \in L^2(\Omega) \times (0, T]$, for any $t > 0$, find $u(\cdot, t) \in H_0^1(\Omega)$, $u_t \in L^2(\Omega)$ such that

$$(u_t, v) + a(u, v) = (f, v) \text{ for all } v \in H_0^1(\Omega). \quad (\text{B.2})$$

We then refine the weak formulation (B.2). The right hand side could be generalized to $f \in H^{-1}(\Omega)$. Since Δ map $H_0^1(\Omega)$ to $H^{-1}(\Omega)$, we can treat $u_t(\cdot, t) \in H^{-1}(\Omega)$ for a fixed t . We then introduce the Sobolev space for the time dependent functions

$$L^q(0, T; W^{k,p}(\Omega)) := \{u(x, t) \mid \|u\|_{L^q(0, T; W^{k,p}(\Omega))} := \left(\int_0^T \|u(\cdot, t)\|_{k,p}^q dt \right)^{\frac{1}{q}} < \infty\}.$$

Our refined weak formulation will be : given $f \in L^2(0, T; H^{-1}(\Omega))$ and $u_0 \in H_0^1(\Omega)$, find $u \in L^2(0, T; H_0^1(\Omega))$ and $u_t \in L^2(0, T; H^{-1}(\Omega))$ such that

$$\begin{cases} \langle u_t, v \rangle + a(u, v) = \langle f, v \rangle \quad \forall v \in H_0^1(\Omega), \text{ and a.e. } t \in (0, T), \\ u(\cdot, 0) = u_0. \end{cases} \quad (\text{B.3})$$

APPENDIX B. SOME ESSENTIAL RESULTS ON NUMERICAL ANALYSIS

We assume the equation (B.3) is well posed.

To easy the stability analysis, we treat t as a parameter and the function $u = u(x, t)$ as a mapping

$$u : [0, T] \rightarrow H_0^1(\Omega),$$

defined as

$$u(t)(x) := u(x, t) \quad x \in \Omega, \quad 0 \leq t \leq T.$$

With a slight abuse of the notation, here we still use $u(t)$ to denote the map. The norm $\|u(t)\|$ or $\|u_t\|_1$ is taken with respect to the spatial variable.

We then introduce the differential operator

$$\mathcal{L} : L^2(0, T; H_0^1(\Omega)) \rightarrow L^2(0, T; H^{-1}(\Omega)) \times H_0^1(\Omega)$$

as

$$(\mathcal{L}u)(\cdot, t) = \partial_t u - \Delta u \text{ in } H^{-1}(\Omega), \text{ for } t \in (0, T] \text{ a.e.}$$

$$(\mathcal{L}u)(\cdot, 0) = u(\cdot, 0).$$

Then the equation (B.3) can be written as

$$\mathcal{L}u = (f, u_0).$$

Here we explicitly include the initial condition. Note that the spatial boundary condition is build into the space $H_0^1(\Omega)$

B.3 Finite difference methods for the 1-D heat equation

In this section, we consider a simple 1-D heat equation

$$u_t = u_{xx} + f \text{ in } (0, 1) \times (0, T), \tag{B.4}$$

$$u(0) = u(1) = 0, u(x, 0) = u_0(x). \tag{B.5}$$

to illustrate the main issues in the numerical methods for solving parabolic equations.

Let $\Omega = (0, 1)$ be decomposed into a uniform grid $\{0 = x^0 < x^1 < \dots < x^{N+1} = 1\}$ with $x^i = ih$, $h = \frac{1}{N}$, and time interval $(0, T)$ be decomposed into $\{0 = t^0 < t^1 < \dots < t^M = T\}$ with $t_n = n\delta_t$, $\delta_t = \frac{T}{M}$. The tensor product of these two grids gives a two dimensional rectangular grid for the domain $\Omega \times (0, T)$. We now introduce two finite difference methods by discretizing the equation (B.4) on grid points.

B.3.1 The forward Euler method

We shall approximate the function value $u(x^i, t^n)$ by U_n^i and u_{xx} by second order central difference

$$u_{xx}(x^i, t^n) \approx \frac{U_n^{i-1} + U_n^{i+1} - 2U_n^i}{h^2}.$$

For the time derivative, we use the forward Euler scheme

$$u_t(x^i, t^n) \approx \frac{U_{n+1}^i - U_n^i}{\delta_t}. \tag{B.6}$$

APPENDIX B. SOME ESSENTIAL RESULTS ON NUMERICAL ANALYSIS

Together with the initial condition and the source $F_n^i = f(x^i, t^n)$, we then end with a system

$$\frac{U_{n+1}^i - U_n^i}{\delta_t} = \frac{U_n^{i-1} + U_n^{i+1} - 2U_n^i}{h^2} + F_n^i \quad 1 \leq i \leq N, 1 \leq n \leq M, \quad (\text{B.7})$$

$$U_0^i = u_0(x^i), \quad 1 \leq i \leq N, n = 0. \quad (\text{B.8})$$

To write (B.7) in a compact form, we introduce the parameter $\lambda = \delta_t/h^2$ and the vector

$$U_n = (U_n^1, U_n^2, \dots, U_n^N)^t$$

. Then (B.7) can be written as, for $n = 0, \dots, M$

$$U_{n+1} = AU_n + \delta_t F_n,$$

where

$$A = I + \lambda \Delta_h = \begin{pmatrix} 1 - 2\lambda & \lambda & 0 & 0 \\ \lambda & 1 - 2\lambda & \lambda & 0 \\ \dots & \dots & \dots & \dots \\ 0 & \lambda & 1 - 2\lambda & \lambda \\ 0 & 0 & \lambda & 1 - 2\lambda \end{pmatrix}. \quad (\text{B.9})$$

Starting from $t = 0$, we can evaluate point values at grid points from the initial condition and thus obtain U_0 . After that, the unknown at next time step is computed by one matrix-vector multiplication and vector addition which can be done very efficiently without strong the matrix. This method also called time marching. The first issue is on the stability in time. When $f = 0$, that is, heat equation without source, in the continuous level, the solution should exponential decay. In the discrete level, we have $U_{n+1} = AU_n$ and want to control the magnitude of U in certain norm.

Theorem B.1. *When the time step $\delta_t \leq h^2/2$, the forward Euler method is stable in the maximum norm in the sense that if $U_{n+1} = AU_n$ then*

$$\|U_n\|_\infty \leq \|U_0\|_\infty \leq \|u_0\|_\infty.$$

B.3.2 The backward Euler method

Now we study backward Euler to remove the strong constrain on the time step for the stability. The method is simply using backward difference to approximate the time derivative. We list the system below:

$$\frac{U_n^i - U_{n-1}^i}{\delta_t} = \frac{U_n^{i-1} + U_n^{i+1} - 2U_n^i}{h^2} + F_n^i \quad 1 \leq i \leq N, 1 \leq n \leq M, \quad (\text{B.10})$$

$$U_0^i = u_0(x^i) \quad 1 \leq i \leq N, n = 0. \quad (\text{B.11})$$

In the matrix form (B.10) reads as

$$(I - \lambda \Delta_h)U_n = U_{n-1} + \delta_t F_n. \quad (\text{B.12})$$

Starting from U_0 , to compute the value at the next time step, we need to solve an algebraic equation to obtain

$$U_n = (I - \lambda \Delta_h)^{-1}(U_{n-1} + \delta_t F_n).$$

The inverse of the matrix, which involves the stiffness matrix of Laplacian operator, is not easy in high dimensions. For 1-D problem, the matrix is tri-diagonal and can be solved very efficiently. The gain is the unconditional stability.

Theorem B.2. *For the backward Euler method without source term, that is, $(I - \lambda \Delta_h)U^n = U^{n-1}$, we always have the stability*

$$\|U_n\|_\infty \leq \|U_{n-1}\|_\infty \leq \|u_0\|_\infty.$$

B.4 Finite element method: semidiscretization in space

Let $\{\mathcal{T}_h, h \rightarrow 0\}$ be a quasi-uniform family of triangulations of Ω . The semi-discretized finite element method is: given $f \in \mathbb{V}'_h \times (0, T]$, $u_{0,h} \in \mathbb{V}_h$, find $u_h \in L^2(0, T; \mathbb{V}_h)$ such that

$$\begin{cases} (\partial_t, u_t) + a(u_h, v_h) = \langle f, v_h \rangle, & \forall v_h \in \mathbb{V}_h, t \in \mathbb{R}^+ \\ u_h(\cdot, 0) = u_{0,h} \end{cases} \quad (\text{B.13})$$

The scheme (B.13) is called semi-discretization since u_h is still a continuous function of t . The initial condition u_0 is approximated by $u_{0,h} \in \mathbb{V}_h$ and the choice of $u_{0,h}$ is not unique.

We can expand $u_h = \sum_{i=1}^N u_i(t) \varphi_i(x)$, where φ_i is the standard hat basis at the vertex x_i for $i = 1, \dots, N$, the number of interior nodes, and the corresponding coefficient $u_i(t)$ now is a function of time t . The solution u_t can be computed by solving an ODE system

$$\dot{\mathbf{u}} + \mathbf{A}\mathbf{u} = \mathbf{f},$$

where $\mathbf{u} = (u_1, \dots, u_N)^t$, \mathbf{A} is the stiffness matrix, and $\mathbf{f} = (f_1, \dots, f_N)^t$.

B.5 Finite element method: semidiscretization in time

We consider the semi-discretization in time. We first discretize the time. We first discretize the time interval $(0, T)$ by a uniform grid with size $\delta_t = T/N$ and denote by $t^n = n\delta_t$ for $n = 0, \dots, N$. A continuous function in time will be interpolated into a vector by $(I^n f)(\cdot, t^n) = f(\cdot, t^n)$. Recall that $A = -\Delta : H_0^1 \rightarrow H_0^{-1}$. We list these schemes in operator form.

- Forward Euler. $u_h^0 = u_{0,h}$

$$\left(\frac{u_h^n - u_h^{n-1}}{\delta_t}, v_h \right) + a(u_h^{n-1}, v_h) = \langle f_h^{n-1}, v_h \rangle, \quad \forall v_h \in \mathbb{V}_h, 1 \leq n \leq N.$$

- Backward Euler. $u_h^0 = u_{0,h}$

$$\left(\frac{u_h^n - u_h^{n-1}}{\delta_t}, v_h \right) + a(u_h^n, v_h) = \langle f_h^n, v_h \rangle, \quad \forall v_h \in \mathbb{V}_h, 1 \leq n \leq N.$$

Stability

We write the discretization using operator form and the stability in L^2 norm is very natural. Let $A = -\Delta|_{\mathbb{V}_h}$.

- Forward Euler

$$u_h^n = (I - \delta_t A) u_h^{n-1} + \delta_t f_h^{n-1}.$$

- Backward Euler

$$u_h^n = (I - \delta_t A)^{-1} (u_h^{n-1} + \delta_t f_h^n).$$

Since $A = -\Delta$ is symmetric in the L^2 inner product, to obtain the stability in L^2 norm, we only need to study the spectral radius of these operators.

- Forward Euler

$$\rho(I - \delta_t A) = |1 - \delta_t \lambda_{\max}(A)| \leq 1,$$

APPENDIX B. SOME ESSENTIAL RESULTS ON NUMERICAL ANALYSIS

provided

$$\delta_t \leq \frac{2}{\lambda_{max}(A)}.$$

Note that $\lambda_{max}(A) = \mathcal{O}(h^{-2})$. We need the time step is in the size of h^2 to make the forward Euler stable

- Backward Euler For any $\delta_t > 0$, since A is SPD, that is $\lambda_{max}(A) > 0$

$$\rho((I - \delta_t A)^{-1}) = (1 + \delta_t \lambda_{min}(A))^{-1} \leq 1.$$

Theorem B.3. *For forward Euler, when $\delta_t < \frac{1}{\lambda_{max}(A)}$*

$$\|u_h^n\| \leq \|u_h^0\| + \sum_{k=0}^{n-1} \delta_t \|f_h^k\|.$$

For backward Euler,

$$\|u_h^n\| \leq \|u_h^0\| + \sum_{k=0}^{n-1} \delta_t \|f_h^{k+1}\|.$$

Appendix C

Numerical algorithm: a specific case

As announced above, let us present the code for the test *InitialFunc* – $-Test_1$ discussed at page 26.

```
load "iovtk"//VTK it consists of an open source C++ library for displaying
different types of data
//Pre-processing
```

COMMENT: In the processing phase the mesh function of Freefem ++ automatically generates a mesh of triangles Th on the considered domain which in this case is a square domain.

```
//1.1 Mesh
int n=200; //number of iterations
mesh Th=square(n,n,[4*x-2,4*y-2]);//example of mesh on square domain
```

COMMENT: A finite element space is, usually, a space of polynomial functions on elements. Here $fespace\ V_h$ ($Th, P1$) defines V_h to be the space of continuous functions on each triangle of Th . As it is a linear vector space of finite dimension, basis can be found.

```
//1.2 Fespace and functions(FEM)
//Semi-discretization in space
fespace Vh(Th,P1);
Vh u,ut,uold;
Vh v,vt,vold;
//definition of a called gradient function
macro gradient(u)[dx(u),dy(u)];
```

```
//1.3 Semi-discretization in time and data definition
real t=0;
int N=250;
real dt=1e-4;//1e-4
real k3=0.1;// +u
real k4=1;//-v
real k2=1;//grad(v)
real k1=0.2;//non linear term
func u0=1.15*exp(-x^2-y^2)*(4-x^2)^2*(4-y^2)^2;
//func u0= 24*((x^2-4)^2+(y^2-4)^2 + 1)-0.05*((x^2-4)^4+(y^2-4)^4);
func v0=0.55*exp(-x^2-y^2)*(4-x^2)^2*(4-y^2)^2;
```

```
//2.Processing
uold=u0;
```

APPENDIX C. NUMERICAL ALGORITHM: A SPECIFIC CASE

```

vold=v0;
//plot(vold,uold,value=1,wait=1);//plots of initial data
real intu0 = int2d(Th)(uold);
cout << "intu0=" << intu0 << "(4pi=" << 4*pi <<)" << endl;

problem kellerSegel([u,v],[ut,vt])=
  int2d(Th)( u*ut+dt*gradient(u)*gradient(ut))
  +int2d(Th)(v*vt+k2*dt*gradient(v)*gradient(vt))
  -int2d(Th)(uold*ut+k1*dt*uold*gradient(vold)*gradient(ut))
  -int2d(Th)(vold*vt-k3*dt*vold*vt+k4*dt*uold*vt);

problem kellerSegelV(v,vt)=
  int2d(Th)(
    v*vt+k2*dt*gradient(v)*gradient(vt)
  )
  -int2d(Th)(vold*vt-k3*dt*vold*vt+k4*dt*uold*vt)
  ;

problem kellerSegelU(u,ut)=
  int2d(Th)(
    u*ut+dt*gradient(u)*gradient(ut)
  )
  -int2d(Th)(uold*ut+k1*dt*uold*gradient(vold)*gradient(ut)
  );

//Time interation
real[int] xx(N+1), yymax(N+1), yymin(N+1);
xx[0]=0;
yymax[0]=abs(uold[0].max);
yymin[0]=abs(uold[0].min);

uold=u0;
vold=v0;
//plot(uold,wait=1,dim=3,value=1);

real s0=clock();
int k=0;
savevtk("vtk/kS-" + k + ".vtk", Th, uold,vold, dataname="u v");
real eps0=1.e+4;
real maxu=0;
real minu=0;
while( k<N && maxu<eps0) {
  k++;
  t=t+dt;
  cout<< "iter " << k << ", t = " << t << endl;
  xx[k] = t;
  cout<< ", xx = " << xx[k] << endl;
  kellerSegelU;
  kellerSegelV;
  vold= v;
  uold= u;
}

```

APPENDIX C. NUMERICAL ALGORITHM: A SPECIFIC CASE

```

maxu=u[0].max;
minu=u[0].min;
yymax[k]=abs(maxu);
yymin[k]=abs(minu);
plot(u,dim=3,wait=1,fill=true, value=1);//graph at each iteration
cout<< "max(u) = " <<maxu <<endl;
cout<< "min(u) = " <<minu <<endl;
savevtk("vtk/kelleSegel-" + k + ".vtk", Th, u,v, dataname="u v");
}
if (maxu<eps0)
  cout<<"No hay blow-up para eps0="+eps0+
    " N iter="+k+
    " t="+t <<endl;
else
  cout<<"hay blow-up para eps0="+eps0+
    " N iter="+k+
    " t="+t <<endl;
//plot(u,dim=3,wait=1,fill=true, value=1);
if(1)
  {
    ofstream file("plotmax.txt");
    for (int i=0; i<=k; i++)
      {
        file << xx[i]<< " " << yymin[i] << endl;
      }
  }
{
  ofstream file("plotmin.txt");
  for (int i=0; i<=N; i++)
    {file << xx[i]<< " " << yymin[i] << endl;
    }
}

real s1=clock();
cout << "tempo trascorso " << s1-s0 <<endl;

plot(u,v,dim=3,fill=true,wait=1,value=1);
system("python3 plotmax.py");

```